Critical Reviews in Biotechnology, 21(2):67–110 (2001)

Hydrodynamic Damage to Animal Cells

Yusuf Chisti

Institute of Technology and Engineering, Massey University, Private Bag 11 222, Palmerston North, New Zealand. Telephone: +64-6-356-9099 ext. 2911. Fax: +64-6-350-5604. E-mail address: Y.Chisti@massey.ac.nz

Table of Contents

0738-8551/01/$.50

ABSTRACT: Animal cells are affected by hydrodynamic forces that occur in culture vessel, transfer piping, and recovery operations such as microfiltration. Depending on the type, intensity, and duration of the force, and the specifics of the cell, the force may induce various kinds of responses in the subject cells. Both biochemical and physiological responses are observed, including apoptosis and purely mechanical destruction of the cell. This review examines the kinds of hydrodynamic forces encountered in bioprocessing equipment and the impact of those forces on cells. Methods are given for quantifying the magnitude of the specific forces, and the response thresholds are noted for the common types of cells cultured in free suspension, supported on microcarriers, and anchored to stationary surfaces.

KEY WORDS: animal cell culture, bioreactors cell damage, erythrocytes, shear effects.

I. INTRODUCTION

Human and animal cell cultures are widely used to produce vaccines, therapeutic proteins, and diagnostic antibodies.[1,2] Advances in tissue regeneration from *in vitro* cultured cells promise to further expand the demand for cell culture processes, and additional explosive growth is likely as methods are established for generating functional organs such as heart and kidney from cells.

Cells are delicate. Culture and processing of cells invariably expose them to variously intense hydrodynamic forces. A sufficiently intense force will destroy cells outright, while a force of lesser magnitude may induce various physiological responses, including death, without necessarily causing any obvious physical damage. This review examines the nature of the forces encountered in bioprocessing and the effects of these forces on cells. The discussion considers freely suspended cells and those anchored to suspended microcarriers and stationary surfaces. Following convention, the many kinds of damaging forces are collectively referred to here as "shear forces", even though the damage many not be always attributable to shear stress or shear rate. The focus is only on the damaging phenomena that cannot be ascribed to gas bubbles. The damaging effects of sparging with a gas have been treated comprehensively in several other reviews.[3-9]

II. SHEAR FORCES IN PROCESS EQUIPMENT

Substantial information exists on the effects of hydrodynamic forces on cells in defined flow geometries such as viscometers and capillaries,[3,10-16] but little is known about shear fields in bioreactors[17-19] and other process equipment such as pumps and valves. Whereas selection of more shear-tolerant cell lines can be helpful, successful culture of shear-sensitive biocatalysts requires attention to bioreactor design and operation. In many cases, the need to prevent cell lysis persists beyond the bioreactor culture step and into various stages of downstream processing, even when the cells are not the final product. Unwanted cell lysis makes purification of extracellular secreted products difficult. In addition, stability of an extracellular protein product may be severely compromised by contact with large amounts of proteases that are released from lysing cells.[20,21] Premature lysis may cause other processing problems. One example of shear-related viabil-

ity loss and consequent increase in extracellular protein content of the broth is shown in Figure 1 for downstream recovery of animal cells by microfiltration. The lysis of recombinant BHK cells in Figure 1 was due to shear stress in the microfiltration module. In this specific case, shear-induced lysis led to clogging of filter membrane with cell debris. Similarly, choice of pumps, valves, and flow conditions during various processing steps determines whether cells are harvested undamaged.[5,10]

The magnitude of the fluid mechanical forces is often expressed as shear stress, τ, or shear rate, γ. These quantities are related; thus, in laminar Newtonian flow,

$$\tau = \gamma \mu_L \qquad (1)$$

where μ_L is the viscosity of the fluid. Shear rate is a measure of spatial variation in local velocities in a fluid. Cell damage in a moving fluid is sometimes associated with the magnitude of the prevailing shear rate or the associated shear stress, but these quantities are neither easily defined nor easily measured in the relatively turbulent environment of most process machines. Moreover, shear rate varies with location within a vessel. Attempts have been made to characterize an average shear rate or a maximum shear rate in various types of bioreactors and process flow devices, as discussed next for the more common cases.

A. Gas-Agitated Bioreactors

Bubble columns and airlift devices are the most common types of gas-agitated bioreactors[18] that are used extensively in culturing animal cells.[23-31] The mean shear rate in bubble columns has been generally correlated with the superficial gas velocity[17,19,32] as follows:

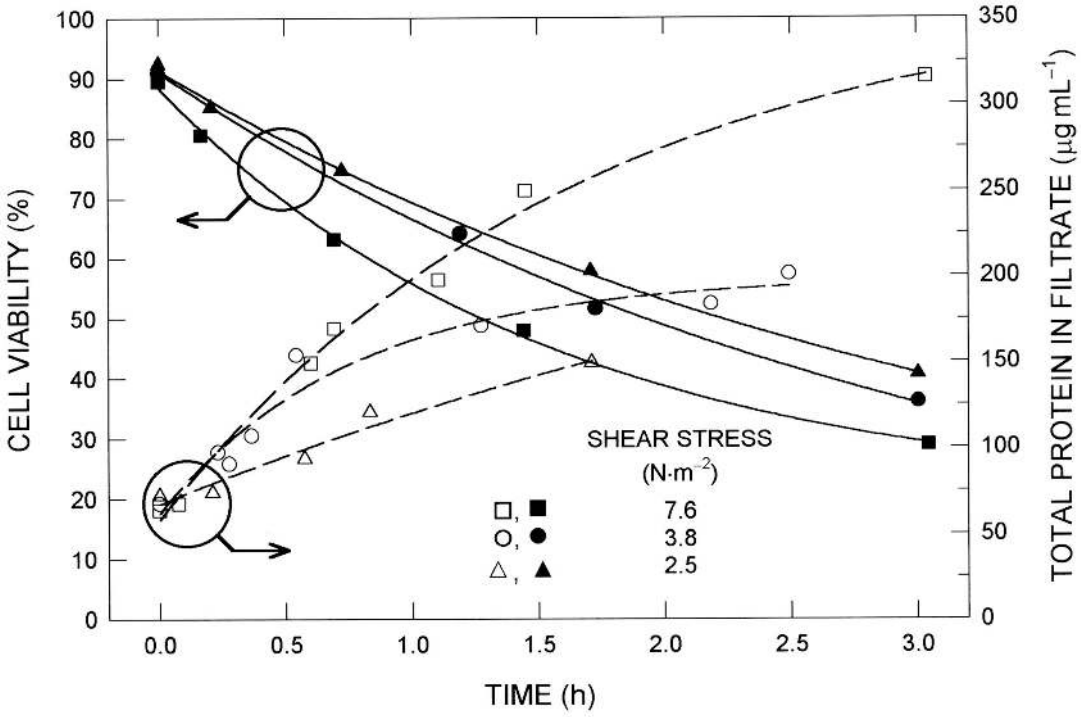

FIGURE 1. Changes in cell viability and extracellular protein content of the broth during microfiltration of recombinant BHK cells at various shear stress levels in the filter module. Flow in the recycle loop and the peristaltic pump used to circulate the broth did not contribute to cell damage. The human interleukin-2 producing BHK cells were cultured in serum free medium without shear protectants. The filtrate flux was constant at 30 $L \cdot h^{-1} \cdot m^{-2}$. (*Source:* Vogel and Kroner.[22])

$$\gamma = kU_G^a \qquad (2)$$

In most cases, the parameter a in Eq. 2 equals 1.0, but the k value varies widely, as noted in Table 1. Consequently, the available equations provide wildly disparate estimates of shear rate as illustrated in Figure 2 for various superficial aeration velocities in air-water system in a bubble column. In many cases, the 'average shear rate' (Table 1) is actually the average at the wall, not the value in the bulk fluid.[12,17-19]

As pointed out elsewhere,[17,19] Eq. 2 has also been incorrectly applied to airlift bioreactors, using the superficial gas velocity in the riser zone as a correlating parameter. A more suitable form of Eq. 2 for airlift reactors is

$$\gamma = \frac{kU_{Gr}}{1 + \frac{A_d}{A_r}} \qquad (10)$$

where U_{Gr} is the superficial gas velocity in the riser, A_r is the cross-sectional area of the riser, and A_d is the cross-sectional area of the downcomer. In addition to the already noted discrepancies (Figure 2), Eq. 2 and Eq. 10 have other significant flaws. The shear rate is also expected to depend on the momentum transfer capability of a fluid, that is, on the density and the viscosity of the fluid, but Eq. 2 and Eq. 10 show no such dependence. Indeed, it is well known that the bubble size in a turbulent field depends on the viscosity and the density of the fluid as well as on the specific energy input rate.[17] Therefore, it is reasonable to assume that correlations that express the shear rate as a function of U_G (or U_{Gr}) alone are incomplete.[19] Furthermore, correlations such as Eq. 2 have generally been based on the observations of phenomena at solid-liquid interfaces (e.g., heat transfer from coils or jackets), and their extension to phenomena at the gas-liquid interface or the bulk fluid is absurd at best. Shear stress

TABLE 1
Average Shear Rate Equations for Bubble Columns

Equation		Range and reference
$\gamma_{av} = 1000\, U_G^{0.5}$	(3)	U_G < 0.04 m·s-1; Nishikawa et al.[33]
$\gamma_{av} = 5000\, U_G$	(4)	0.04 ≤ U_G (m·s-1) ≤ 0.1; Nishikawa et al.[33]
$\gamma_{av} = 1500\, U_G$	(5)	Henzler[34]
$\gamma_{av} = \left(\frac{\rho_L g U_G}{\mu_L} \right)^{0.5}$	(6)	Henzler and Kauling[35]
$\gamma_{av} = 2800\, U_G$	(7)	Schumpe and Deckwer[36]
$\gamma_{av} = \frac{U_G}{d_T}$	(8)	d_T = 0.2 m; Kawase and Moo-Young[37]
$\gamma_{av} = \left(10.3\, n^{-0.63}\right)^{1/(n+1)} \left(\frac{\rho_L g U_G}{K} \right)^{1/(n+1))}$	(9)	Kawase and Kumagai[38]

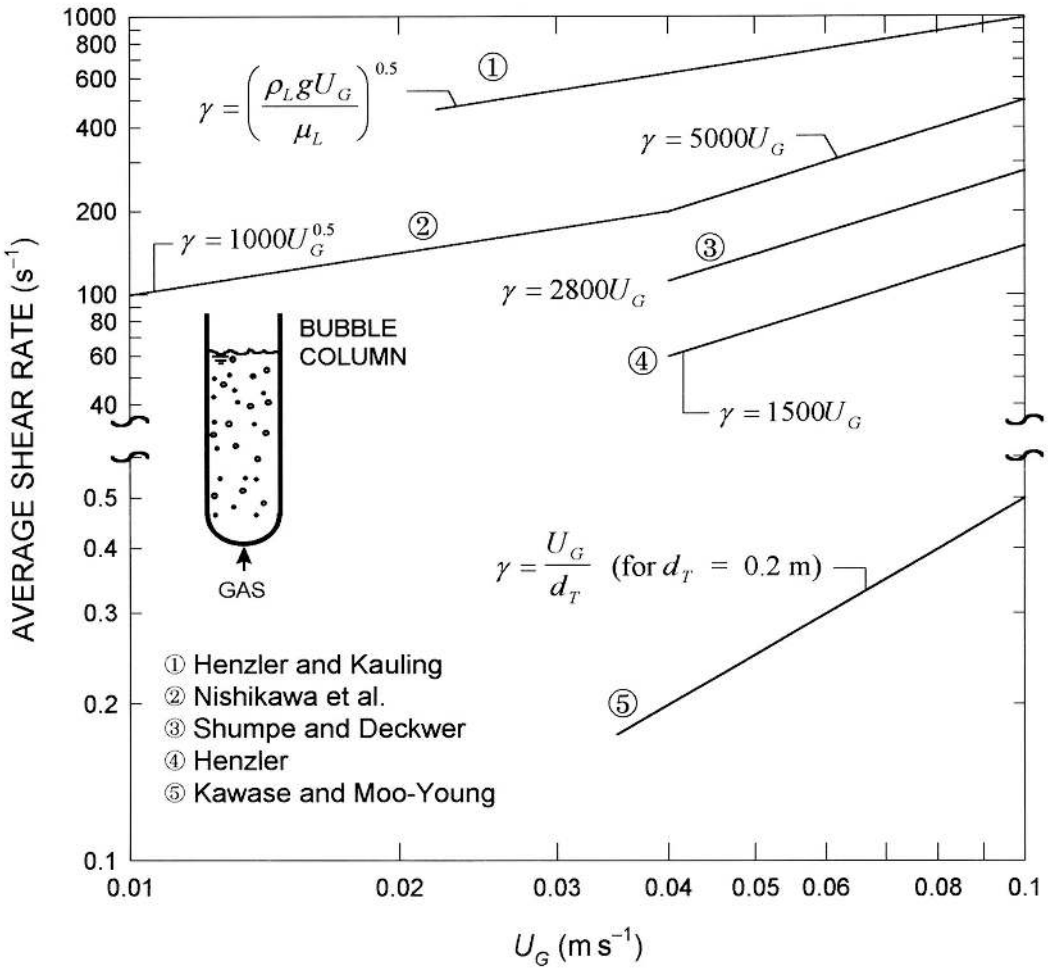

FIGURE 2. Average shear rate in air—water system in a bubble column according to various sources. (Based on Chisti.[5,17])

and hence shear rate at walls of riser and downcomer zones of an airlift device are readily calculated using methods developed for pipes and channels, as discussed later in Section II.C.

Another equation for estimation of an 'effective' shear rate in airlift reactors is

$$\gamma = 3.26 - 3.51\times10^{2} U_{Gr} + 1.48\times10^{4} U_{Gr}^{2} \quad (11)$$

which was developed for $0.004 < U_{Gr}$ (m·s^{-1}) < 0.06;[32] the shear rate range covered was 2 to 35 s^{-1}. Equation 11 was developed in an external-loop airlift reactor. First, the effect of viscosity on the induced liquid circulation velocity in the downcomer was established using Newtonian glycerol solutions at various gas flow rates. The maximum Reynolds number in the downcomer was about 3200, or barely in the turbulent regime. In a second step, pseudoplastic media were used in the reactor, and the effective viscosity (μ_{ap}) of these fluids in the circulation loop was determined as being equal to the viscosity of the Newtonian glycerol solutions, when the two systems were at identical aeration rates and liquid circulation rates. The effective viscosity and the known values of K and n were used in the power law equation to calculate the prevailing shear rate:

$$\gamma = \left(\frac{\mu_{ap}}{K}\right)^{\frac{1}{n-1}} \quad (12)$$

The calculated shear rates were correlated with the superficial gas velocity in the riser, as noted in Eq. 11.[32] Although written in terms of the superficial gas velocity in the riser, Eq. 11 may usefully be expressed in terms of the specific power input in the reactor, as recommended elsewhere.[19]

Because the procedure used[32] in developing Eq. 11 equated the viscosity-associated reduction in the liquid circulation velocity in different fluids, it gave in some sense a shear rate in the vicinity of the interface between the fluid and the walls of the reactor;[17,19] shear rate in the bulk flow, which is the quantity of interest in most cases, was not quantified. Furthermore, the method of analysis used[32] applies strictly to a laminar flow regime, quite unlike the flow situations encountered in most practical operations.

Compared with bubble columns, Eq. 11 yields quite low values for shear rates in airlift reactors as noted by Shi et al.[32] In such comparisons, care needs to be taken to ensure that the devices are being compared at identical values of specific power inputs.[17,19] Although Shi et al.[32] did not adhere to this criterion, the specific geometry of the reactor they used was such that the error was small. Unlike what the authors concluded, Eq. 11 is not suitable for correlating mass transfer from gas bubbles or suspended solids, because it does not give shear rates at gas-liquid or particle-liquid interfaces. Similarly, the usefulness of the shear rate calculated using Eq. 11, for correlating survival of fragile biocatalysts, remains questionable.

Following a methodology identical to that of Shi et al.[32] but in a 0.7 m^3 external-loop airlift device, Al-Masry[39] obtained the equation

$$\gamma_w = 14.9 + 11.1 U_{Gr} + 24.392 \times 10^3 U_{Gr}^2 \qquad (13)$$

for A_d/A_r of unity in a 1.6-m-tall reactor operated such that the superficial gas velocity in the riser remained below 0.07 $m \cdot s^{-1}$.[39] The wall shear rate values were almost always less than 120 s^{-1}. Equation 13 is subject to the same criticisms as Eq. 11. To account for effects of reactor geometry, Al-Masry[39] correlated their data and that of Shi et al.[32] with the equation

$$\gamma_w = 3.36(1 - U_{Gr})^{-32.56}\left(1 + \frac{A_d}{A_r}\right)^{0.89} h_D^{0.44} \qquad (14)$$

which applied to $0.0018 \le U_{Gr}$ ($m \cdot s^{-1}$) ≤ 0.07; $0.11 \le A_d/A_r \le 1.0$; and $1.4 \le h_D$ (m) ≤ 6. Equation 13 and Eq. 14 disregard effects of momentum transport properties on shear rate even though such effects are known to exist.[35,38,40,41]

An alternative, mechanistic approach to quantifying the bulk shear rate in various zones of airlift bioreactors has been advanced by Grima et al.[12] Because the hydrodynamic environment in various zones of airlift reactors tends to be quite different, characterization of shear rate by a single global value is not sensible. The overall shear rates can be deceptively low, even though damaging levels may be experienced in the high-shear zones;[12] hence, the approach of Grima et al.[12] is preferred. This method computes shear rates using reliable expressions for energy dissipation in various zones of airlift reactors.[17,42]

Some directly measured shear rated data in an airlift bioreactor for hybridoma culture have become available.[43] At aeration power input of ~9 $W \cdot m^{-3}$ in the BSA-supplemented medium (BSA concentration = 1 $g \cdot L^{-1}$), the mean shear rate values in the downcomer were ~100 s^{-1} and were independent of height.[43] For the same conditions, the mean wall shear rate values in the riser zone varied axially from a high of ~600 s^{-1} at 0.06 m from the sparger to ~100 s^{-1} about midway up the riser. Measured average wall shear rate values were reduced by BSA supplementation, but this effect was largely independent of the BSA concentration over the range 0.1 to 1.0 $g \cdot L^{-1}$. Although the BSA concentration over the range 0.1 to 1.0 $g \cdot L^{-1}$ did not further affect the mean wall shear rate value, the concentration affected the probability distribution of the shear rates 0.06 m above the

sparger: higher concentrations produced narrower distributions.[43] These results were obtained in a concentric draft-tube airlift device that was sparged in the draft-tube. The aspect ratio of the vessel was ~7 and the A_r/A_d ratio was ~0.7. Significantly, these observations regarding the axial variation in the mean wall shear rate (γ_w) do not agree with Eq. 14 which predicts a hyperbolic increase in γ_w with increasing height h_D of dispersion.

Other attempts at characterizing the hydrodynamic forces have focused on the structure of turbulence[44] in water and power law solutions (K = 0.0194 Pa·s$^{0.973}$ and 0.0596 Pa·s$^{0.958}$) in an external-loop airlift reactor. The reactor achieved complete gas-liquid separation, and there was no gas in the downcomer. Measurements of local root mean square velocity fluctuations as an indicator of turbulence intensity showed a slight decrease from the center of the riser to the wall. These measurements were at a constant gas velocity of 2.05×10^{-2} m·s^{-1}. The magnitudes of the velocity fluctuations were similar for all media; however, the velocity fluctuations were much lower in the gas-free downcomer than in the riser despite similar values of Reynolds numbers in the two zones. Based on measurements of one-dimensional energy spectra in the center of the riser,[44] turbulence could not be considered isotropic, particularly in power law fluids. Other evidence also supports a lack of isotropic turbulence in airlift and bubble column reactors under typical conditions of operation[45,46] and at the scales of interest.

B. Mechanically Stirred Vessels

Mechanically stirred bioreactors are widely used to culture animal cells.[2,47-57] The local velocity at a fixed position in a stirred bioreactor fluctuates around a mean value, hence the shear rate fluctuates. In the discharge streams of a Rushton turbine (Figure 3), the fluctuating component of the local velocity increases with the rotational speed of the impeller. The magnitude of fluctuations depends on the specific location in the tank, the type of impeller, the agitation speed, and the properties of the fluid. In tanks with radial flow impellers such as Rushton turbines, the velocity fluctuations are greatest near the impeller tip and decline rapidly as one moves radially outward from the tip. Elsewhere in the vessel, the velocity fluctuations are reduced yet further. Because of these factors, several different characteristic shear rate values may be identified, including

FIGURE 3. Rushton turbine.

the time-averaged mean shear rate, the maximum shear rate at the impeller, and the shear rate in the region swept by the impeller blades. Some of the expressions for estimating the various shear rates are summarized in Table 2.

The available shear rate correlations are compared in Figure 4 for water in a standard stirred tank[60] agitated with a 0.1-m-diameter six-bladed Rushton turbine. For some context, the shear rate around a rising bubble may be approximated as the ratio of the terminal rise velocity to the bubble diameter (or radius); hence,

$$\gamma_{av} = \frac{2U_B}{d_B} \tag{23}$$

In air-water, under conditions typical of bubble columns and airlift reactors, the bubble rise velocity U_B is about 0.2 m·s^{-1}, and the bubble diameter d_B is about 0.006 m. Thus, the interfacial shear rate approximates to 67 s^{-1} if the interface is nonmobile. Lower shear rates are expected at circulating interfaces. Under some conditions, the turbulence field in a mechanically agitated vessel may be locally isotropic. When this happens, the equations in Table 2 still provide useful estimates of maximum and the average bulk shear rate values, but the shear rate associated with the fluid microeddies also becomes an important consideration as discussed in Section II.E.

In perfusion culture of suspended animal cells, 'spinfilters' (Figure 5), or rotating cylinders made of wire mesh, are sometimes used to retain cells in the bioreactor. The wire screen openings are significantly larger (e.g., 25 μm) than the cells, which are retained by a hydrodynamic mechanism requiring rapid rotation (e.g., 500 rpm) of the spinfilter. The cell-free spent medium is withdrawn from the zone within the rotating screen. Rotation of spinfilters does not generally damage animal cells.[62] The cell-free zone within the rotating screen is sometimes used for aeration by sparging. Shear effects may become important in other designs of perfusion devices.[63]

C. Pipework and Flow Channels

Flow in pipes and channels occurs commonly during the transfer of culture between bioreactors, while harvesting, and during recovery processes such as microfiltration and ultrafiltration.[21,22,47,64] Cell culture broths almost always behave as Newtonian fluids. The broth viscosity is typically close to 0.75×10^{-3} Pa·s.[52,65,66] In developed laminar flow of a Newtonian fluid through a straight tube of diameter d, the shear rate at the wall depends on the mean flow velocity, U_L, as follows:

$$\gamma_w = \frac{8U_L}{d} \tag{24}$$

For a rectangular channel of height h, the maximum or wall shear rate in developed laminar flow is

$$\gamma_w = \frac{6U_L}{h} \tag{25}$$

where U_L is again the mean flow velocity.

The wall shear stress (i.e., the maximum value) in a flow channel such as the riser of an airlift reactor is related to the pressure drop (ΔP), the length L of channel, and the hydraulic diameter;[18] thus,

$$\tau_w = \frac{d}{4L}\Delta P \tag{26}$$

Consequently, in turbulent flow, the wall shear stress is

$$\tau_w = \frac{1}{2} C_f \rho_L U_L^2 \tag{27}$$

where ρ_L is the liquid density and C_f is the Fanning friction factor. The latter is related with the Reynolds number as follows

$$C_f = 0.0792\left(\frac{\rho_L U_L d}{\mu_L}\right)^{-0.25} \tag{28}$$

TABLE 2
Shear Rate Equations for Stirred Vessels

Equation	Applicability and reference
1. Time-averaged mean shear rate $\gamma_{av} = 4.2N\left(\frac{d_i}{d_T}\right)^{0.3}\frac{d_i}{W}$ (15)	Six-bladed Rushton turbine agitating a Newtonian fluid in a baffled vessel. Bowen[58]
2. The time-averaged maximum shear rate $\gamma_{max} = 2.3\gamma_{av}$ (16) where γ_{av} is obtained from Eq. 15	Six-bladed Rushton turbine agitating a newtonian fluid in a baffled vessel. Bowen[58]
3. Maximum shear rate at impeller blade $\gamma_{max} = 3.3N^{1.5}d_i\left(\frac{\rho_L}{\mu_L}\right)^{1/2}$ (17) The coefficient is uncertain within ±20% of the noted value.	Rushton turbine; Newtonian and non-Newtonian liquids when $100 \le \left(Nd_i^2\rho_L/\mu_L\right) \le 29{,}000.$ For non-Newtonian fluids, μ_L in Eq. 17 is the zero shear viscosity. Robertson and Ulbrecht[41]
4. Maximum shear rate at impeller blade $\gamma_{max} = N(1+5.3n)^{1/n}\left(\frac{N^{2-n}d_i^2\rho_L}{K}\right)^{1/1+n}$ (18)	Rushton turbine; Newtonian and non-Newtonian media. Wichterle et al. cited by Robertson and Ulbrecht[41]

TABLE 2 (continued)

5. Average shear rate $\gamma_{av} = k_i \left(\frac{4n}{3n+1} \right)^{n/n-1} N$ (19) Eq. 19 is a modified form of the well-known Metzner and Otto equation, $\gamma_{av} = k_i \cdot N$.		A broad range of impellers; Newtonian and non-Newtonian media.[59] In Eq. 19, k_i is an impeller-dependent constant. Some typical k_i values are 11–13 for 6-bladed disc turbines; 10–13 for paddle impellers; ~7 for paddles with curved blades; ~10 for propellers; and ~30 for helical ribbon impellers.[60]
6. Average shear rate $\gamma_{av} = \frac{0.367}{\mu_L} \left[\frac{P_T}{V_L} \left(\frac{V_L}{V_s \mathrm{Po}} \right)^{0.42} \right]^{0.55}$ (20) where the Power number, Po, is $\frac{P_T}{\rho_L N^3 d_i^5}$		The original equation was expressed in terms of average shear stress, τ. $1 \leq \tau$ (N·m-2) ≤ 40. Hoffmann et al.[40]
7. Average shear rate $\gamma_{av} = \left(\frac{P_T}{V_D \mu_{ap}} \right)^{0.5}$ (21)		Henzler and Kauling cited by Candia and Deckwer[61]
8. Shear rate in the region around the impeller $\gamma_I = \left[0.038 \frac{P_T}{V_L K} \left(\frac{d_T}{d_i} \right)^3 \frac{d_i}{h_b} \right]^{1/1+n}$ (22)		Rushton turbine-type impellers. Obernosterer and Henzler cited by Candia and Deckwer[61]

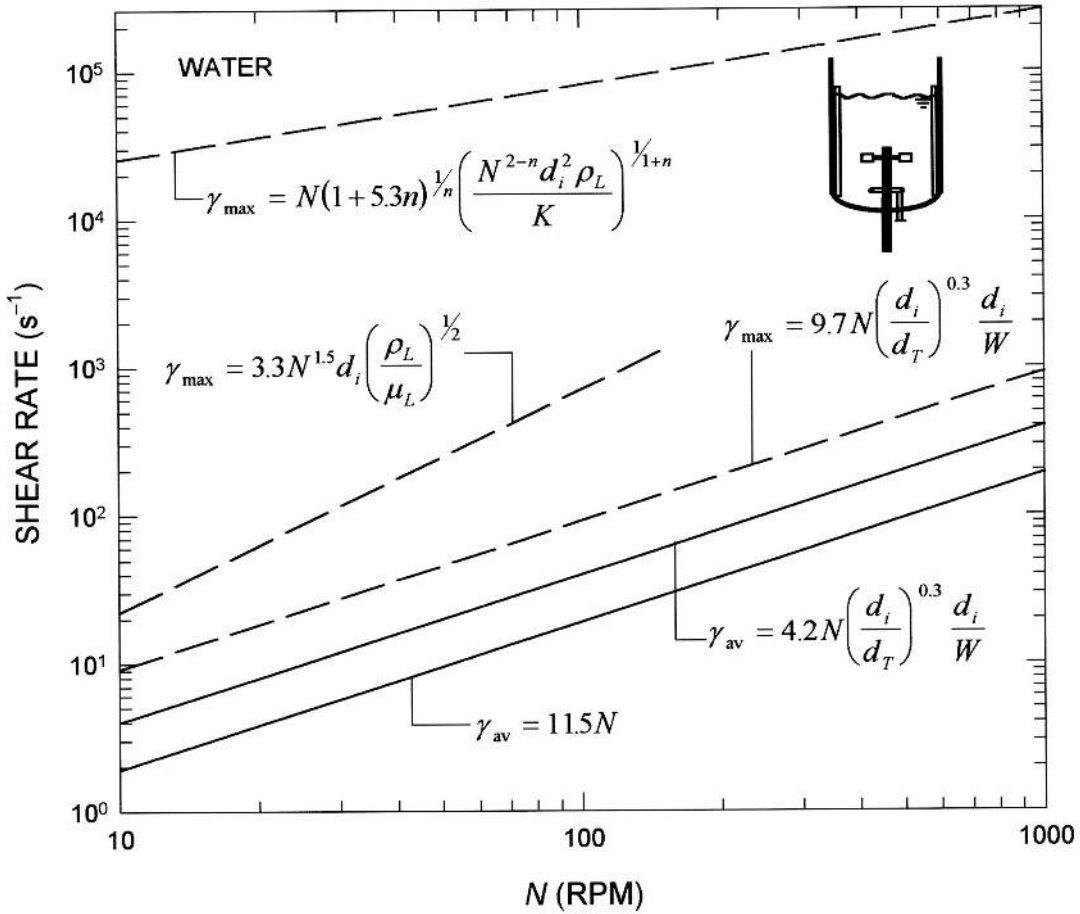

FIGURE 4. Comparison of the various shear rate correlations for water in a standard stirred tank agitated with a 0.1-m-diameter 6-bladed Rushton turbine. The dashed lines are for the maximum shear rate; the solid ones are for the average shear rate. (See text for additional details.)

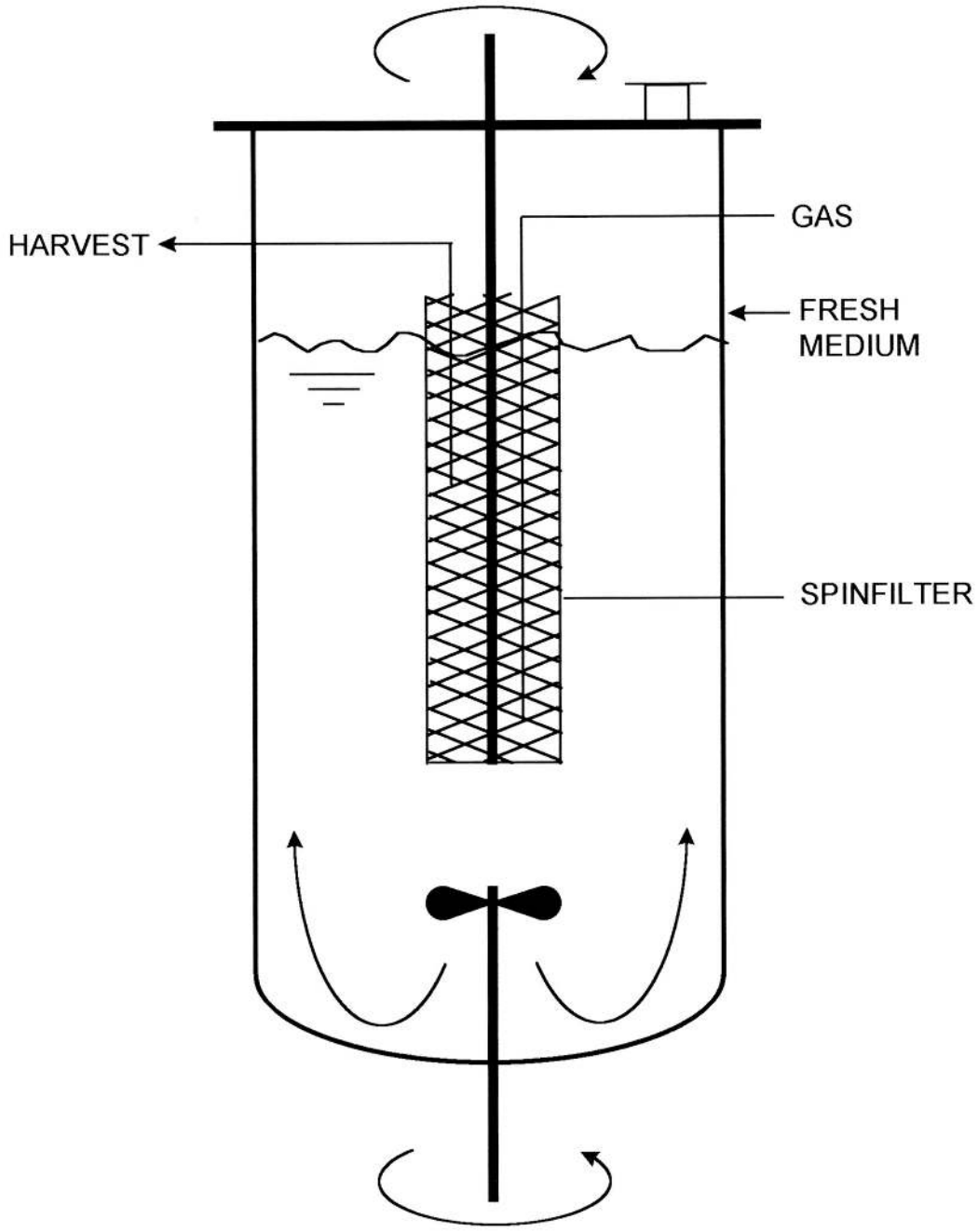

FIGURE 5. Perfusion culture with spinfilter for hydrodynamics-based cell retention in bioreactors.

In Eq. 28, d is the hydraulic diameter of the flow channel or pipe. From Eq. 27 and Eq. 28, the wall shear stress can be shown to depend on Newtonian viscosity of the fluid $\tau_w \propto \mu_L^{-0.75}$.[12] A typical variation of the wall shear rate and the isotropic turbulence shear rate (see Section II.E) during flow of a cell culture broth through a pipe is shown in Figure 6. The wall shear rate greatly exceeds that in the bulk fluid, nonetheless, as discussed in Section II.E, conditions in the bulk volume are usually the relevant ones with regard to cell damage. Use of Eq. 24 and Eq. 27 and others given later that are similar presupposes that the liquid velocity is known. This is normally the case in pipes and channels; however, in airlift bioreactors the induced liquid circulation rate will often need to be estimated using published methods.[17,18,42]

D. Turbulent Jets

A submerged jet forms wherever a pipe or nozzle discharges a fluid beneath the surface of the same fluid in a larger vessel. For example, culture broth recirculating from a tank to a microfiltration unit and back to the tank could form a submerged jet. If the cross-sectional area of the discharge nozzle is less than about 25% of that of the reservoir, the wall effects

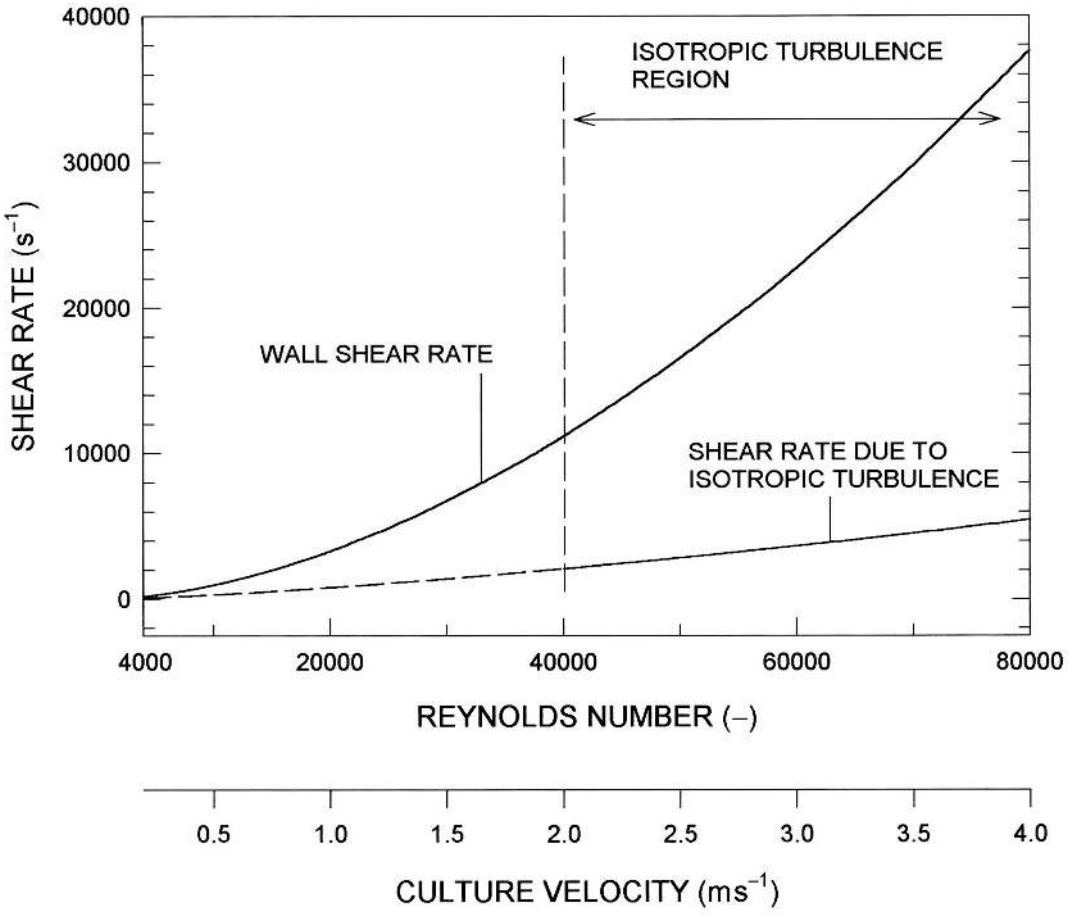

FIGURE 6. Variation of shear rate at pipe wall and in the bulk culture during turbulent flow through a 0.02-m-diameter smooth pipe at various Reynolds numbers. The culture velocity is also shown. Density and viscosity of the culture fluid were 10^3 kg·m^{-3} and 10^{-3} Pa·s, respectively. Turbulence was considered to be isotropic when the length scale of the terminal microeddies was smaller than or equal to a thousandth of the diameter of the pipe. The latter was taken as the scale of the primary eddy.

can be neglected and the jet is said to be 'free.' A jet is turbulent when the Reynolds number at the orifice exceeds about 3000. In a stable submerged turbulent jet, the maximum shear stress occurs in the direction of discharge, six to seven nozzle diameters downstream from the orifice. This shear stress is given as

$$\tau_{\max J} = 0.018\rho_L u_o^2 \tag{29}$$

where u_o is the velocity at the orifice.

A turbulent jet consists of two regions (Figure 7). A conical core of fluid next to the orifice retains the discharge velocity of the orifice. This region of potential flow extends about six nozzle diameters from the discharge orifice, and within this region shear stresses are minimal. The potential core is surrounded by an expanding zone of developed turbulence. Quiescent fluid surrounds the turbulent flow field (Figure 7). The total mass flow rate at any cross-section in the turbulent flow field of a jet increases linearly with distance from the orifice, as the surrounding quiescent fluid is entrained in the jet. The velocity profile in the turbulent region is Gaussian and it is described by the equation

$$\frac{u_l}{u_{\max}} = e^{-\beta\left(r/x\right)^2} \tag{30}$$

where β is about 75.2, r/x is the dimensionless radial distance (Figure 7), u_l is the local velocity at position r, and $u_{\max}$ is the maximum or the centerline velocity. The Gaussian profile persists until the centerline velocity declines to that of the surrounding flow. The maximum velocity, $u_{\max}$, depends on the exit velocity at the nozzle and the axial distance:

$$\frac{u_{\max}}{u_o} = C\left(\frac{d}{x}\right) \tag{31}$$

In Eq. 31, d is the orifice diameter, x is the axial distance, and the constant C is about 6.06. The constants β and C may be influenced by the operating conditions.

If the nozzle discharge velocity is the same as in the pipe, the maximum shear stress at the pipe wall is always less than in the jet. The ratio of these shear stresses is given as

$$\frac{\tau_{\max J}}{\tau_w} = 0.455\left(\frac{\rho_L U_L d}{\mu_L}\right)^{0.25} \tag{32}$$

The ratio $\tau_{\max J}/\tau_w$ increases with increasing velocity of discharge, as shown in Figure 8 for discharge of a cell culture fluid from a 0.02-m-diameter pipe. Consequently, damage to frag-

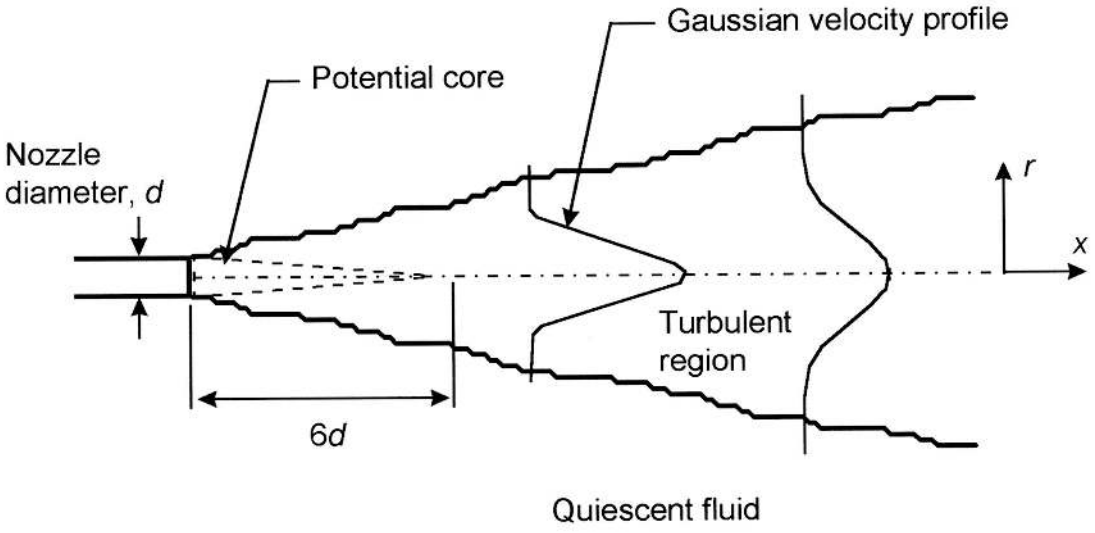

FIGURE 7. A submerged turbulent jet.

ile cells may occur during transfer operations such as inoculation of a bioreactor even though the velocity in the transfer pipe may be relatively low. These effects can be avoided by discharging the jet above the level of the receiving fluid such that the liquid flows down the vessel wall.

Energy dissipation rates in turbulent jets are nonuniform. Dissipation is greatest near the axis of the jet and declines radially outward, becoming negligible at dimensionless radial distances (*r/x*) of greater than 0.2. In the fully developed turbulent region, the radially averaged energy dissipation rate E declines with axial location as follows:

$$E = \eta\left(\frac{d\ u_o}{x^{4/3}}\right)^3 \tag{33}$$

where the constant η is about 50.[67,68]

E. Shear Phenomena in Isotropic Turbulence

A turbulence field in any process equipment is said to be isotropic when the size of the primary eddies generated by the turbulence causing mechanism is a thousandfold or more compared with the size of the energy dissipating microeddies. Depending on the situation, the length scale of the primary eddies may be approximated as the width of the impeller blade or the diameter of the impeller in a stirred tank. In bubble columns and airlift bioreactors, the length scale of primary eddies is approximated as the diameter of the column (or the riser tube), or the diameter of the bubble issuing from the gas sparger;[5,18] the latter approach is preferred because a rising bubble is the primary source of turbulence in most gas-agitated bioreactors.

Shear stress, shear rate, the dimensions of microeddies, and other characteristics of flow are ultimately determined by the energy input and dissipation rates in the fluid. The local shear rate in the vicinity of an eddy in an isotropically turbulent field may be estimated as the ratio of the velocity and the length of the eddy; hence,

$$\gamma_i = \frac{u}{\ell} = \frac{\mu_L}{\rho_L \ell^2} \tag{34}$$

where ρ_L and μ_L are, respectively, the density and the viscosity of the fluid. The mean length, ℓ, and the velocity, u, of the microeddies are related with the specific energy dissipation rate E in the turbulence field; thus,

$$\ell = \left(\frac{\mu_L}{\rho_L}\right)^{3/4} E^{-1/4} \tag{35}$$

and

$$u = \left(\frac{\mu_L E}{\rho_L}\right)^{1/4} \tag{36}$$

Generally, all the energy imparted to a fluid is dissipated in microeddies, and E equals the rate of energy input. Equations 34 to 36 apply when local isotropic turbulence prevails.

For single-phase pipe flow, the specific energy dissipation rate is

$$E = \frac{U_L \Delta P}{\rho_L L} \tag{37}$$

where ΔP is the pressure drop over the tube length L, and U_L is the mean flow velocity. The pressure drop may be computed using the earlier noted Eqs. 26 to 28. The energy dissipation rate in bubble columns and airlift vessels is a function of the superficial aeration velocity;[17,18] thus

$$E = gU_G \qquad \text{(bubble columns)} \tag{38}$$

and

$$E = g\frac{U_{Gr}}{1 + \dfrac{A_d}{A_r}} \qquad \text{(airlift bioreactors)} \tag{39}$$

Methods for calculating the specific energy dissipation rate in stirred vessels have been discussed elsewhere.[60,69] The mean energy dissipation rate in an unaerated vessel is given as

$$E = \frac{\mathrm{Po}N^3 d_i^5}{\mathrm{V_L}} \tag{40}$$

where Po is the power number, d_i is the diameter of the impeller, and N is the rotation speed (s^{-1}). In developed turbulent flow in stirred vessels, that is, when the impeller Reynolds number ($Nd_i^2 \rho_L/\mu_L$) exceeds 10^4, the power number is generally constant for a given type of impeller and tank geometry. The constant Power number values are noted in Table 3 for some common types of impellers in baffled stirred tanks. The energy dissipation rate in the presence of aeration is generally less than in the equivalent ungassed state. The extent of reduction depends on the aeration rate used. In typically aerated conditions in microbial culture, the energy dissipated is generally 50 to 60% of the nonsparged case; however, in animal cell culture the aeration rates are so small that power number is barely affected by aeration.

The local energy dissipation varies greatly from the mean value in a stirred tank. The maximum energy dissipation occurs in the vicinity of the impellers and this maximum value can be calculated using the equation

$$E = \mathrm{Po}N^3 d_i^2 \tag{41}$$

Equation 41 assumes that dissipation occurs in the volume around the impeller, but it disregards flow through that volume. If the volume flowing through the impeller zone in 1 s is taken into account, the maximum specific energy dissipation will reduce by a factor that depends on the rotational speed and the geometry of the impeller.

As noted in Figure 9, the same relationship exists between the isotropic turbulence shear rate and the specific energy dissipation rate in various culture devices; however, because the different devices operate in different ranges of specific energy dissipation rates, the shear rates experienced by cells are different under typically used culture conditions. Generally, if a biocatalyst particle is much smaller than the calculated length, ℓ, of the microeddies, the particle is simply carried around by the fluid eddy, without experiencing any disruptive force. In contrast, a particle that is larger than the length scale of the eddy will experience pressure differentials on its surface. The resulting force may kill or rupture the cell. Turbulence within the fluid is only one factor contributing to cell damage in a bioreactor. Other damage-causing phenomena are interparticle collisions; collisions with walls, other stationary surfaces, and the impeller; shear forces associated with bubble rupture at the surface of the fluid;[3-6,8] phenomena linked with bubble coalescence, breakup, and rise;[70,71] and bubble formation at the gas sparger. Some of these damaging phenomena are discussed in other sections of this

TABLE 3
Turbulent Power Number in Baffled Stirred Tanks

Impeller	Po (—)
Propeller (square pitch, 3-bladed)	0.32
45° Pitched blade turbine (6-blades, pumping down)	1.90
Lightnin' A310 hydrofoil	0.31
Turbine (6-bladed)	6.30
Turbine (6-curved blades)	4.80
Flat paddle (2-blades)	1.70
Scaba agitator	1.45
Prochem impeller (5-blades, $d_i = d_T/2$)	1.0

Source: Chisti and Moo-Young.[60]

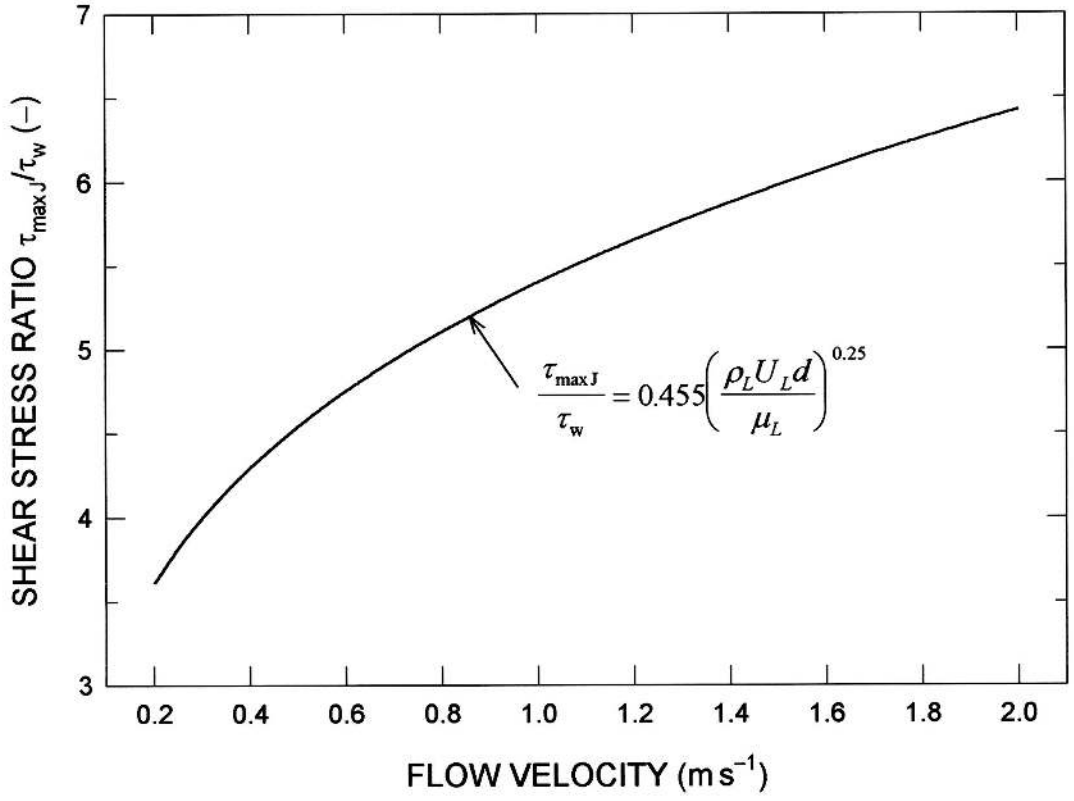

FIGURE 8. Ratio of the maximum shear stress in the jet to that at pipe wall for flow of animal cell culture fluid (density = 10^3 kg·m^{-3}, viscosity = 10^{-3} Pa·s) from a 0.02-m-diameter pipe ending in same diameter opening to form a free jet.

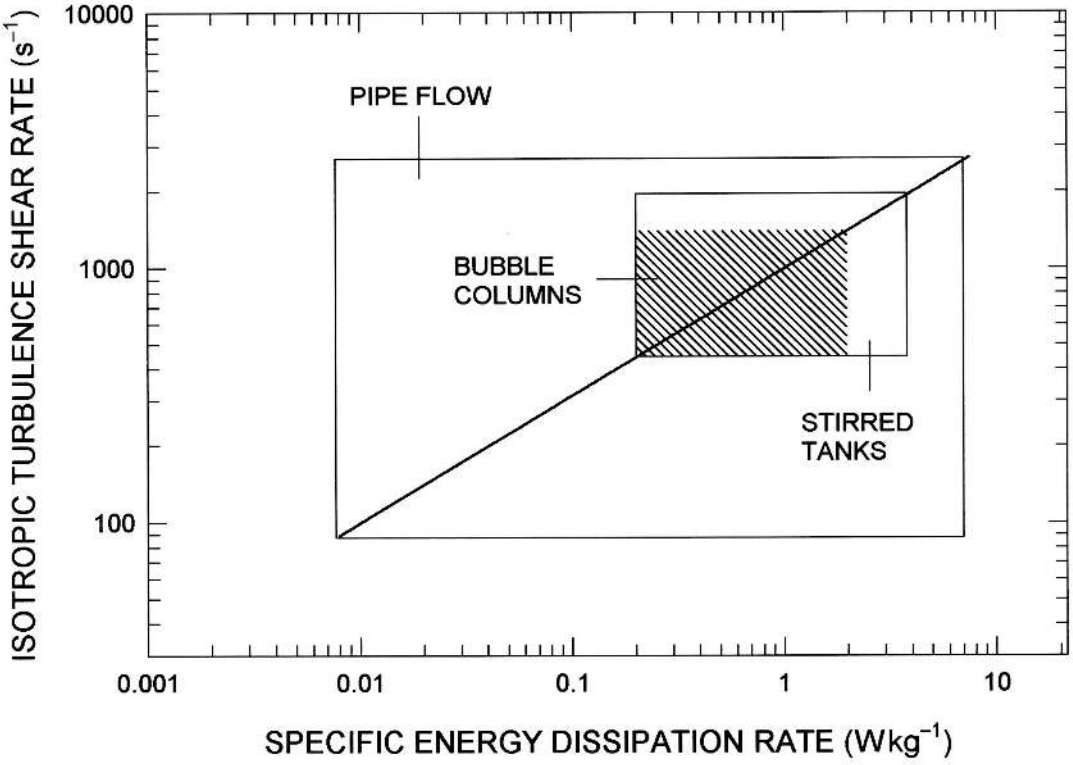

FIGURE 9. The relationship between isotropic turbulence shear rate and the specific energy dissipation rate is the same (solid line) in various culture devices, but the devices operate in different ranges of specific energy dissipation rates (boxes) along the diagonal line. The plot is for a water-like culture fluid (10^3 kg·m^{-3} density, 10^{-3} Pa·s viscosity).

article. Other approaches to calculating shear stresses in turbulent flow are discussed by Cherry and Kwon.[72]

Summarizing, several possible shear rate values may be calculated for a given situation in a bioprocess device. Not every calculated value is appropriate or relevant to the problem at hand. For pneumatically agitated bioreactors, when the turbulence characteristics in the bulk fluid are the relevant ones, the preferred approach is to use Eq. 34 for shear rate in the vicinity of eddies. The same applies to mechanically stirred tanks. In flow systems such as pipes and channels, the shear rate at the wall is always greater than in bulk flow (Figure 6); nevertheless, the shear rate in the bulk fluid is generally the more relevant with regards to cell damage. There are two reasons for this: (1) because of hydrodynamic forces cells typically move away from the walls; and (2) a relatively high shear rate in laminar flow of the boundary layer adjacent to walls is less damaging than a similar shear rate in turbulent flow away from walls.[5] In some cases, the relevant shear rate may be that at the interface of a rising bubble unless turbulence is so intense that bubbles do not rise freely. Other situations would be controlled by the bubble rupture events,[3,4,6,8,73] as discussed later. In yet other cases, the fluid eddy shear rate and the maximum shear rate at the impeller will need to be taken into account. Factors such as the frequency of passage of a sensitive biocatalyst through a high shear region may need to be considered for cyclic flows such as occur in stirred tanks, airlift devices, and recycle loops.

F. Effects of Suspended Particles on Turbulence

Suspended particles such as cells and microcarriers themselves modulate turbulence. These effects are complex[74] and depend on the ratio of the particle diameter d_p and the length of the energy-containing eddy, ℓ_e. Small particles follow the fluid flow, and some of the turbulent energy is transformed into the particles' kinetic energy.[75] When d_p/ℓ_e is smaller than 0.1, the particle dissipates energy and turbulence is dampened. Larger particles ($d_p/\ell_e >$ 0.1) enhance small-scale turbulence through wakes induced by their relative velocity with respect to the fluid.[75] How much turbulence is enhanced or dampened depends on the system, not on the magnitude of d_p/ℓ_e. When the concentration of solids in suspension exceeds 20 to 30% (by vol), the dominant mechanism affecting the flow is particle-particle interactions and not particle-fluid interactions.[75] In microcarrier culture of animal cells, the volume fraction of solids is typically less than 10%, but higher concentrations may occur in processes such as the expanded bed chromatography of the whole broth.[20]

III. SHEAR EFFECTS ON CELLS

A. Suspended Cells

1. Hybridomas and Suspension-Adapted Cells

Freely suspended animal cells in bubble-free bioreactors are not damaged by mechanical agitation even at intensities much greater than the ones used in typical processing. Exceptions occur in extensional or elongational flow in certain high-shear devices even when the flow is laminar.[76,77] Extensional or elongational flow is produced whenever the cross-sectional area of the flow channel reduces (e.g., at an orifice on the wall of a tank or at the entrance of a capillary connected to a larger reservoir). The fluid elements undergoing extensional flow stretch and thin. Suspended particles also experience elongational forces in the direction of flow and compression perpendicular to the flow streamlines. Drops subjected to extension flow can rupture. Although no cell is a homogeneous fluid, suspended animal cells such as granulocytes and hybridomas behave similar to drops in a shear field. Rupture of

erythrocytes at entrances to capillaries is well known.[76] Similarly, extensional flow through orifices of high-pressure homogenizers contributes to breakage of even the very robust microbial cells.[78] The likelihood of damage in an extensional flow field is reduced if the cell can rotate or tumble to relax the imposed stress. Indeed, hydrodynamic stress alone is an insufficient criterion for quantifying cell damage,[76,77] and the possibility of rotation-associated stress relaxation also needs to be considered. Strain relaxation by tumbling motions is well-documented for erythrocytes in viscometric flows.[76] Shear effects on suspended erythrocytes are discussed in detail in Section III.A.2.

Based on the hypothesis that a cell should burst whenever its bursting membrane tension is exceeded in a flow field, Born et al.[11] developed a model for predicting cell damage in laminar flow. The model relied on the cell's separately measured mechanical properties such as burst strength. The medium-suspended hybridoma cell was modeled as a drop—an approach that has been used previously to analyze damage to suspended erythrocytes. The undeformed 'drop' had the same diameter as that of the hybridoma. The interfacial tension between the drop and the medium was taken to equal the membrane tension of the cell. The viscosity of the drop was taken to be the internal viscosity of the hybridoma. The latter was assumed to have a constant value of 3.5×10^{-3} Pa·s, as similar values have been reported for cytosolic viscosity of the red blood cells. However, the precise value of the viscosity was not critical to predicting the extent of cell damage in a shear field.[11]

A cell behaving as a drop suspended in a laminar flow field will deform to a degree determined by the shear rate, the viscosity of the suspending fluid, and the elastic area compressibility modulus of the cell.[11] At a certain shear stress for a given cell, the bursting membrane tension will be exceeded, and that cell will be destroyed or otherwise damaged.[11] The deformation d_f of an initially spherical drop exposed to laminar shear is defined as

$$d_f = \frac{x - y}{x + y} \tag{42}$$

where x and y are the lengths of the major and minor axes, respectively, of the deformed ellipsoidal drop (Figure 10). According to Taylor,[79] the deformation depends on the shear rate; thus,

$$d_f = \varphi \gamma \mu_L \frac{d_p}{2\sigma} \tag{43}$$

where μ_L is the viscosity of the suspending fluid, d_p is the diameter of the original drop, γ is the shear rate, and σ is the interfacial tension. The parameter φ depends on the viscosity of the drop[79] as follows:

$$\varphi = \frac{\frac{19}{16}\frac{\mu_d}{\mu_L} + 1}{\frac{\mu_d}{\mu_L} + 1} \tag{44}$$

In Eq. 44, μ_d is the viscosity of the drop phase. Based on Taylor's[79] Eq. 43 for drops, Born et al.[11] propounded that the membrane tension σ in a cell exposed to laminar shear rate γ should be

$$\sigma = \varphi \gamma \mu_L \frac{d_p}{2d_f} \tag{45}$$

and the cell would burst if $\sigma \geq \sigma_B$, where σ_B, the membrane tension at cell burst,[11] can be determined by micromanipulation methods.[80] Because laminar shear stress τ equals $\gamma \cdot \mu_L$, the cell burst condition may be expressed as:[11]

$$\frac{\varphi \tau d_p}{2d_{fb}} \geq \sigma_B \tag{46}$$

In expression 46, d_{fb} is the deformation at cell burst. The d_{fb} has been related to the increase in the cell surface area at the burst event;[81] thus,

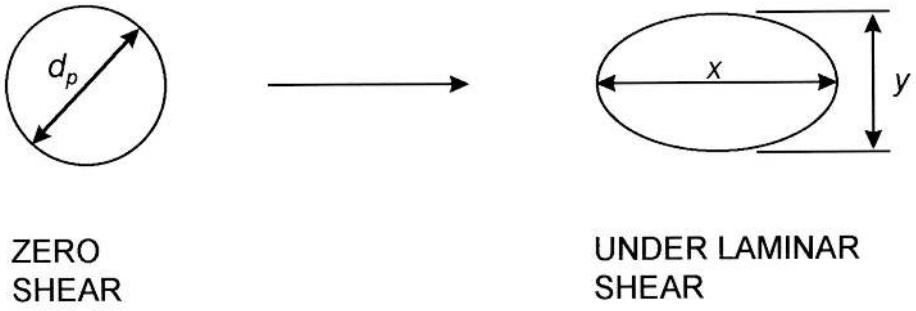

FIGURE 10. Deformation of a spherical cell, behaving as a drop, on exposure to laminar shear stress.

$$\frac{\Delta A_B}{A_o} = 0.5\theta^{2/3} + 0.5\theta^{-1/3}\frac{\arccos\theta}{\sqrt{1-\theta^2}} - 1 \qquad (47)$$

where

$$\theta = \frac{1-d_{fb}}{1+d_{fb}} \qquad (48)$$

In Eq. 47, ΔA_B is the increase in cell surface area at burst and A_o is the surface area of the original undeformed cell. The ratio $\Delta A_B/A_o$ is an intrinsic property of a cell and can be determined through micromanipulation;[80] hence, d_{fb} can be established. Equations 47 and 48 are based on the assumption that the cell deforms into a prolate ellipsoid (Figure 10). The deformation, d_{fb}, is a weak function of the relative increase in the cell surface area and an average value of d_{fb} can be used[11] in Eq. 47.

The membrane burst tension has a Gaussian distribution with a mean and standard deviation of σ_{Bm} and σ_{Bs}, respectively. Similarly, the initial cell diameter in the absence of deformation also has a Gaussian distribution with a mean diameter and standard deviation of d_{pm} and d_{ps}, respectively. The mean values and standard deviations of diameters and burst tensions can be determined by micromanipulation.[11] Because the burst tension, σ_B, takes a Gaussian form, its distribution can be normalized by transforming to the variable $q = (\sigma_B - \sigma_{Bm})/\sigma_{Bs}$.[11] For all cells of a given diameter d_p, the percentage of rupture P_τ at some shear stress τ is obtained[11] by evaluating the integral

$$P_\tau = \int_{-\infty}^{Z} \frac{1}{\sqrt{2\pi}} e^{-q^2/2} dq \qquad (49)$$

where

$$Z = \frac{\dfrac{\varphi\tau d_p}{2d_{fb}} - \sigma_{Bm}}{\sigma_{Bs}} \qquad (50)$$

For cells of different diameters, the expected fraction of burst cells, P_B, is obtained[11] by evaluating the integral

$$P_B = \int_{-\infty}^{\infty} \frac{1}{\sqrt{2\pi}} e^{-p^2/2} P_\tau dp \qquad (51)$$

Equation 51 accounts for the Gaussian distribution of cell size. In Eq. 51, p is the normalized cell diameter[11] given as

$$p = \frac{d_p - d_{pm}}{d_{ps}} \qquad (52)$$

Resistance to rupture of an animal cell appears to vary with age and so does the size of cells such as hybridomas. According to Born et al.,[11] the mean bursting tension σ_{Bm} of murine hybridomas depended on the cell age in batch culture: σ_{Bm} increased from about 1.5 mNm^{-1} at ≤ 20 h to about 2 mNm^{-1} at 80 h.[11] During this period, the mean cell diameter declined slightly; however, changes in cell diameter and burst tension were apparently

unrelated.[80] Through the culture period, the mean value of the $\Delta A_B/A_o$ ratio was about 2.[11] Born et al.[11] noted that the percent disruption predicted by the model compared well with the experimental data for various levels of applied laminar shear stress in a cone-and-plate viscometer.

The cell damage model of Born et al.[11] implies that a cell exposed a certain laminar shear stress is either disrupted or it remains unaffected; thus, cell loss is predicted to be independent of the duration of exposure. In theory, the model should allow a prediction of the cell survival behavior from mechanical property data measured by micromanipulation. Born et al.[11] provide some evidence in support of their model, but its broader applicability remains questionable in view of the many nonconforming observations.[82-84] As pointed out in Section III.B.2, a cell will experience debilitating damage and effective loss of function long before damaging forces reach the threshold of physical destruction. Consequently, unless there is a direct and identifiable relationship between loss of function prior to physical rupture and the rupture threshold conditions, the practical utility of the approach propounded is limited at best. Also, cells sheared in a cone-and-plate device experience different levels of shear stress depending on how far they are from the apex of the cone. Indeed, cells nearer the apex have been observed to undergo severe deformations, while those near the edge of the cone may be little affected.[76]

For a hybridoma line, Born et al.[11] reported that exposure to laminar shear stress (208 $N \cdot m^{-2}$) in unaerated flow in a cone-and-plate viscometer led to substantial loss in cell count and viability within 20 min. At a constant 180-s exposure, increasing shear stress over 100 to 350 $N \cdot m^{-2}$ linearly enhanced cell disruption, with >90% of the cells being destroyed at 350 $N \cdot m^{-2}$ stress level.[11] Shear stress levels of the order of 100 to 300 $N \cdot m^{-2}$ do occur during bubble rupture at the surface of a bioreactor.[85] In view of the reported observations,[11] similarly high values of shear stress also damage hybridomas in *unaerated* laminar flow.

Shear stress related damage to a mouse-mouse hybridoma was examined by Abu-Reesh and Kargi[82] under laminar and turbulent conditions in a coaxial cylinder Searle viscometer. Cells were exposed to 5 to 100 $N \cdot m^{-2}$ shear stress levels for 0.5 to 3.0 h. At a given shear stress and exposure time, turbulent shear was much more damaging than laminar shear[82] as also reported in the past[83] for protozoa and plant cells.[86] Under turbulent conditions, damage occurred when shear stress exceeded 5 $N \cdot m^{-2}$.[82] Respiratory activity of the cells was damaged earlier than the cell membrane, thus implying transmission of the stress signal to the interior of the cell. Cell damage followed first-order kinetics both in laminar and turbulent environments. For turbulent shear stress levels of 5 to 30 $N \cdot m^{-2}$, the death rate constant (k_d) increased exponentially with increasing stress level; the k_d values varied over 0.1 to 1.0 h^{-1}. In coaxial cylinder viscometers with a gap width w and an inner cylinder of diameter d_i rotating at peripheral speed U_T, the laminar-turbulent flow transition is defined by Taylor number (Ta) that is given as

$$\mathrm{Ta} = \left(\frac{\rho_L U_T w}{\mu_L}\right)\left(\frac{2w}{d_i}\right)^{0.5} \tag{53}$$

The flow is laminar when Ta < 41.3. Laminar flow with Taylor vortices occurs when 41.3 < Ta < 400. Fully developed turbulent flow obtains when Taylor number exceeds 400. Abu-Reesh and Kargi[82] varied the rotational speed of the inner cylinder and the viscosity of the suspending fluid to attain different values of Taylor number. The viscosity was varied by adding 2000 kDa dextran.

For hybridoma cells separately grown in continuous culture at various specific growth rates, Petersen et al.[87] concluded that shear sensitivity in a Couette viscometer at a constant shear rate of 5000 s^{-1} was independent of growth rate or of the metabolic state for cells from exponential growth phase. The same cell line was more sensitive to viscometric shear during

lag and stationary phases. This behavior contrasts with that of microbial cells that generally become increasingly shear sensitive as the specific growth rate increases.[78] The latter behavior is associated with poorer development of cell walls in faster growing cells, but animal cells do not have walls and this possibly explains the different behavior.

For a suspended mouse myeloma line in turbulent capillary flow, McQueen et al.[13] noted a threshold average wall shear stress value of 180 $N \cdot m^{-2}$ when lysis first commenced. Although the flow caused lysis, it had no effect on viability,[13] suggesting that cells at various growth stages were equally affected. The sudden flow contraction at the entrance to the capillary may have contributed to cell lysis, but the residence time in the capillary also had an effect at otherwise constant average wall shear stress level. The rate of lysis was first-order in cell number. Above the threshold shear stress value, the specific lysis rate increased with increasing level of shear stress.[13] The growth rate and the DNA synthesis rate of the cells exposed to the shearing environment were unaffected when the surviving cells were returned to a normal quiescent growth environment.[13] In other studies cited by McQueen et al.,[13] the shear stress threshold for damage has been reported as 0.87 $N \cdot m^{-2}$ for a mouse hybridoma and 1.5 $N \cdot m^{-2}$ for insect cells. Higher shear sensitivity of another mouse cell line relative to a human carcinoma has been reported.[10]

For human cervical carcinoma HeLa S3 and mouse abdominal fibroblast L929, Augenstein et al.[10] observed lysis of suspended cells in turbulent flow through stainless steel capillaries. Cell death could be correlated with the average wall shear stress level or the power dissipation within the capillaries. The L929 line was more sensitive than the human cell. Control experiments showed that the positive displacement pumps used to circulate the cells through capillaries contributed little to cell lysis.[10] Average wall shear stress levels of $(0.1\text{-}2.0) \times 10^3$ $N \cdot m^{-2}$ were sufficient to induce cell inactivation for the two lines. According to Shiragami,[15] the mean shear stress acting on cells suspended in capillary flow is the shear stress at the capillary walls, so long as the ratio of the cell's diameter to that of the capillary is <0.08.

For a hybridoma examined by Shiragami,[88] the specific rate of monoclonal antibody production in a surface aerated spinner flask depended on the agitation speed. In a 250-mL spinner vessel an agitation rate of ~180 rpm gave the highest specific antibody production rate. The specific productivities were reduced at higher or lower values of agitation speed. The increased antibody production with increasing agitation was associated supposedly with enhanced secretion in a more turbulent environment.[88] Oxygen transfer effects may have better explained the observations (see Ref. 66), but no data were reported on this aspect.

Damage to murine hybridomas was observed by Jan et al.[62] in stirred tanks equipped with marine impellers agitated at sufficiently high speeds that vortexing occurred and gas entrained into the medium. Even at these high speeds, damage could be prevented by baffling the tank, which suppressed vortex formation. Usually though, vortexing is not a problem in large-scale cell culture. Unbaffled, marine impeller-stirred tanks were used successfully by Chisti[47] in industrial culture of several hybridoma lines. Effects of agitation on hybridoma culture in the absence of sparging or surface entrainment were further examined by Smith and Greenfield.[55] Culture growth was unaffected by agitation intensity (100 or 600 rpm) in the RPMI medium supplemented with fetal bovine serum (10% vol/vol). However, in PFHM II medium supplemented with either Pluronic F68, fetal bovine serum, or bovine serum albumin, and agitated at 600 rpm (impeller tip speed = 1.6 $m \cdot s^{-1}$, power input = 1 $kW \cdot m^{-3}$) the results were different: the agitation intensity did not affect the exponential growth rate, but once growth had ceased, the decline phase was substantially faster than in control experiments.[55]

Using steady-state continuous culture of a hybridoma in a surface aerated baffled vessel

stirred with a paddle impeller, Abu-Reesh and Kargi[89] showed that agitation tip speeds up to ~0.7 $m \cdot s^{-1}$ did not damage cells in a medium supplemented with 15% (vol/vol) horse serum. At a lower serum concentration of 7.5%, impeller tip speeds of ~0.5 $m \cdot s^{-1}$ damaged cells and the specific death rate increased with increasing impeller tip speed. Whether any gas entrainment or vortexing occurred was not clear. In media with 7.5% serum, increasing dilution rate over 0.02 to 0.50 h^{-1} reduced the viable cell concentration at constant impeller tip speeds of 0.21 $m \cdot s^{-1}$ and 0.52 $m \cdot s^{-1}$.[89] The agitation-associated damage was first order in cell number. An insect cell line (*S. frugiperda*, Sf9) was more prone to damage. In unaerated stirred cultures, the specific growth rate declined noticeably as the tip speed of standard Rushton turbine increased over 0.24 to 0.94 $m \cdot s^{-1}$ in parallel batch experiments.[90] At 0.70 $m \cdot s^{-1}$ tip speed in paired batch cultures, the growth rate was slightly faster in a marine impeller stirred vessel than in one agitated with a standard Rushton turbine.[90]

Elias et al.[48] subjected quiescent environment cultured human erythrocytic leukocytes to agitation (120 min) in 250-mL Bellco spinner flasks and characterized cell damage as a function of agitation speed of the suspended 42-mm-diameter magnetic bar agitator. The agitation tip speeds tested were 0.105, 0.21, and 0.315 $m \cdot s^{-1}$. Relative to static T-flask culture, the viable cell count as measured by dye exclusion was only marginally reduced at 0.210 and 0.315 $m \cdot s^{-1}$ tip speeds; however, the cells subjected to these agitation speeds (120 min) failed to proliferate on transfer to a quiescent environment.[48] In contrast, cells that had not been agitated, or agitated only at 0.105 $m \cdot s^{-1}$, grew normally when transferred to a static environment. The cells were cultured in RMPI 1640 supplemented with 10% fetal bovine serum. Thus, in some cases at least, turbulence in the absence of aeration does apparently damage cells even under typically used culture conditions, but the damage may go unnoticed because of the limitations of the dye exclusion methodology[91] unless growth profiles are recorded over a significant period. According to Elias et al.,[48] microscopic observations revealed significant damage to actin cytoskeletal network of cells exposed to 0.21 $m \cdot s^{-1}$ (120 min) impeller speed.

Cells grown in FBS-supplemented media, when exposed to a previously nondamaging agitation speed of 0.105 $m \cdot s^{-1}$ in the absence of 10% FBS, failed to proliferate on transfer to a complete medium.[48] At a higher agitation speed of 0.21 $m \cdot s^{-1}$, supplementation with serum failed to protect cells. These observations were interpreted in terms of the turbulence dampening effect of serum. For otherwise equivalent conditions, the addition of 10% FBS to RPMI 1640 medium reduced turbulence as indicated by reduced root mean square velocity fluctuations measured by laser doppler anemometry.[48] Similarly, FBS supplementation reduced turbulent shear stresses in the fluid as shown in Figure 11.[48] In another study, supplementation of the culture medium with BSA reduced the average wall shear stress in an airlift device.[43] This effect was largely independent of the BSA concentration over the range 0.1 to 1.0 $g \cdot L^{-1}$; however, BSA stimulated the hybridoma cell growth only at concentrations of 0.4 $g \cdot L^{-1}$ or greater.[43] (Note: 1 $g \cdot L^{-1}$ protein is equivalent to about 2% (vol/vol) serum; therefore, 0.2 to 2.0% serum may be sufficient to reduce turbulence in boundary layers next to a ridged surface.) Because growth stimulation did not occur until a concentration of 0.4 $g \cdot L^{-1}$, whereas turbulence was dampened at a lower concentration, and the damaging effect was independent of concentration, the turbulence dampening alone may not be a sufficient explanation for the observed improved growth.

The precise nature of the protective effect of serum is not clear; however, in view of the measurements,[43,48] supplementation with sufficient serum clearly dampens turbulence and several authors have suggested this to be the survival enhancing mechanism of serum.[51,92,93] Nevertheless, available data[43] do not support the turbulence-dampening effect as the sole

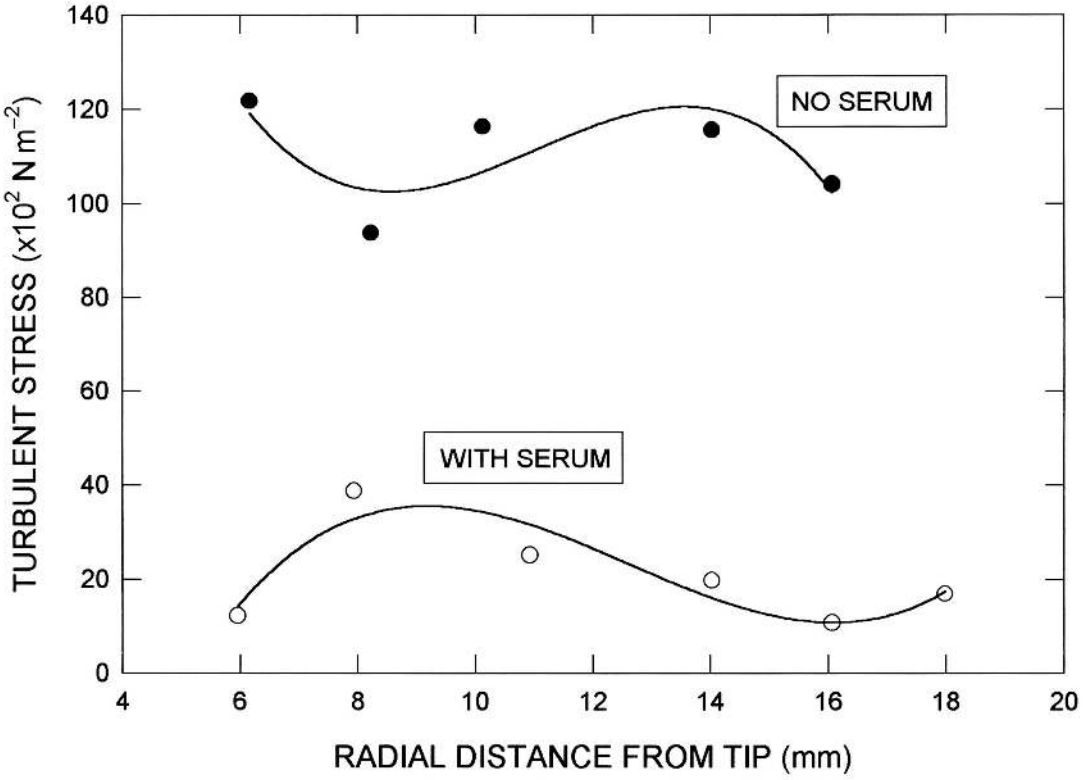

FIGURE 11. Effect of 10% FBS supplementation on turbulent stresses in a 250-mL spinner vessel. The impeller agitation speed was 5 rps (~0.7 m·s^{-1} tip speed). Stress is shown as a function of the radial distance from the impeller tip. (Based on Elias et al.[49])

contributor to improving survival and other biochemical factors also appear to play a role.[94] Indeed, other evidence suggests a lack of relationship between the amount of protection afforded by the serum and enhancement of viscosity,[95,96] the factor responsible for dampening of turbulence.

Intense mechanical forces may produce purely physical damage to cells leading to necrotic death or lysis. In addition, evidence is emerging that otherwise sublethal stress levels may induce a biochemical death mechanism or apoptosis involving active participation of the cell in the death process.[97,98] In gas-free stirred vessel, Al-Rubeai et al.[97] observed no apparent damage to hybridomas in serum-containing media agitated at power inputs of 1.5 W·m^{-3}. Cells lost viability when the energy dissipation rate increased to 350 W·m^{-3}. Necrosis was a significant mechanism of death, but there was also evidence of apoptosis. Apoptosis, a genetic-level self-destruct mechanism programmed into cells, involves synthesis or activation of preexisting hydrolytic enzymes such as proteases and endonucleases. Enzymatic action destroys essential proteins and DNA, leading ultimately to cytoskeletal collapse. In principle, chemical regulatory additives and environmental controls may be used to suppress or postpone apoptotic response, hence helping to improve culture performance under intense hydrodynamic stress. Additives such as Pluronic F-68 and linoleic acid have shown shear protective effects on insect cells (*S. frugiperda*, Sf9) and murine hybridomas in bubble-free agitation.[99,100]

A certain level of hydrodynamic shear is generally beneficial to culture processes, especially in intraparticle immobilized culture where mass transfer limitations can be severe.[66] In producing engineered tissue of smooth muscle cells/polymer matrices (biodegradable 2-mm-diameter fibers of polyglycolic acid assembled into a non-

woven matrix), Kim et al.[101] noted that seeding of the matrix under agitation led to significantly higher intramatrix cell densities than when cells were seeded under static conditions. Moreover, the higher cell densities were attained more rapidly than the lower densities of static culture. In addition, the relative rates of synthesis of elastin and collagen were significantly greater in seeded matrices cultured with agitation than in ones grown statically.[101] A lower possible supply of oxygen or other nutrient may have reduced the performance of static seeding methodology. In view of the above-referenced studies and similar others, sufficiently intense fluid mechanical forces other than those associated with aeration do affect cells. Table 4 provides a summary of the damaging thresholds of impeller tip speed and specific power input for several kinds of suspended cells.

2. Blood Cells

Studies of shear effects on blood cells are relevant in blood banking, processing, and transfusion. Also, shear susceptibility of cells has important implications in the development of certain diseases and the design of biomedical devices such as artificial heart valves and heart-lung machines. Mammalian erythrocytes, or red blood cells, are the best studied of animal cells.[5,76,102] Erythrocytes and leukocytes (white blood cells), being suspended cells *in vivo*, likely experience the kind of stresses encountered in bioreactors and various other industrial processing devices; hence, these cells may provide a broad general insight into mechanical behavior of other cells of mammalian origin. Indeed, suitably chosen erythrocytes have been recommended as a standard cell for comparative assessment of the damaging potential of various hydrodynamic environments.[103] Because eryth-

TABLE 4
Damaging Threshold Values of Impeller Tip Speed or Specific Power Input for Some Animal Cells

Stirred bioreactors	Impeller tip speed ($m \cdot s^{-1}$)
Human erythrocytic leukocytes (serum supplemented)	≤0.21
S. frugiperda Sf9 (unaerated)	<0.7
Several hybridomas	>1 (axial flow impellers)
Hybridoma in stationary phase (no sparging)	~1.6 $m \cdot s^{-1}$ impeller tip speed or power input of 1 $kW \cdot m^{-3}$
Hybridoma (serum-supplemented 15% vol/vol, surface aerated)	≥0.7
Hybridoma as above (serum-supplemented 7.5%, surface aerated)	≤0.5
Hybridomas, serum-containing media, gas-free stirred vessel	power inputs of <350 $W \cdot m^{-3}$
Airlift bioreactors	**Power input ($W \cdot m^{-3}$)**
Vero cells on microcarriers, medium with 10% serum	>2.6
Bubble columns	**Power input ($W \cdot m^{-3}$)**
Myeloma, serum-supplemented medium	~0.42

rocytes do not multiply *in vitro*, the effects of cell damaging forces are not masked by growth-associated adaptation, changes in cell size, and stages of growth.

Erythrocytes are highly deformable cells that orient in laminar flow so that least possible surface area of the disk-shaped cell is perpendicular to the flow (Figure 12). The cytoplasm of erythrocytes is a viscous Newtonian fluid.[102] The cell membrane behaves as an elastic solid: the cell deforms but almost instantly recovers its shape when the deforming force is removed. The membrane has little resistance to bending, but substantially resists increase in area.[102] Erythrocytes suspended in turbulent isotonic saline (viscosity ~1×10^{-3} Pa·s) have been observed to undergo elongation and deformation; however, the cell appears to be less vulnerable to turbulent shear stress than a cell at the same stress level in a viscous suspending medium.[76] (This observation apparently contrasts with the behavior reported for many other cells for which turbulent shear stress generally has been more damaging than equivalent laminar shear stress.[82,83,86]) At a constant shear stress, in laminar viscometric flow, erythrocytes stretch or elongate more as the viscosity of the suspending fluid increases and, consequently, more cells lyse over a fixed time interval (Figure 13). Tumbling motions of cells contribute greatly to relaxing the imposed stresses. Based on measurements in turbulent jets, a critical lytic shear stress level of 4000 $N \cdot m^{-2}$ has been reported for very brief exposures (~10^{-5} s).[76] Measurements on erythrocytes of different mammals reveal that the critical shear stress increases dramatically as the cell volume declines. This is consistent with expectations: the dimensions of fluid eddies capable of causing damage reduce as the cell becomes smaller. Note that shear stress is directly proportional to the shear rate, whereas the eddy size is proportional to $\gamma_i^{-0.5}$ (Eq. 34).

According to Blackshear and Blackshear,[76] a red cell membrane subjected to stress increases in area and lysis occurs when the area is increased by approximately 6.4%. Hemolysis is associated at least in part with physical factors and flow, which produce the hemolysis threshold strain in membranes of erythrocytes.[76] Once the threshold strain is exceeded, membrane pores open and the membrane eventually tears.[76] A briefly (e.g., 1×10^{-2} s) imposed uniaxial tension of 0.058 $N \cdot m^{-1}$ is a sufficient criterion for lysis.[76] When the cell is subjected to biaxial stress, a tension of about 0.029 $N \cdot m^{-1}$ may produce lysis. In viscometric stress for prescribed periods, time to lysis declines as the imposed stress is increased. However, it has been shown conclusively that shear stress alone is not a sufficient predictor of hemolysis rate or thresholds;[76] cell shape and tumbling also play a role.

Erythrocytes allowed to adhere to a glass surface and then subjected to a fluid shear commence movement when the fluid shear force exceeds about 10^{-11} N.[102] During this process the cell gradually moves downstream, but the membrane may remain attached to the surface.[102] The membrane can be deformed permanently when the deforming force persists for more than a few minutes.[102] Shear elasticities of nonnucleated mammalian red cells are generally similar, but elasticities are about an order of magnitude greater for cells of nucleated species. Small amounts of thiol reagents are known

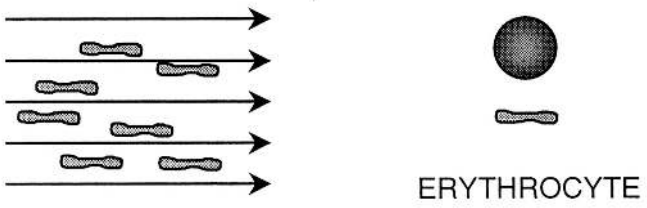

FIGURE 12. Alignment of nonspheroidal cells (e.g., erythrocytes) in laminar flow to minimize surface area projected to flow.

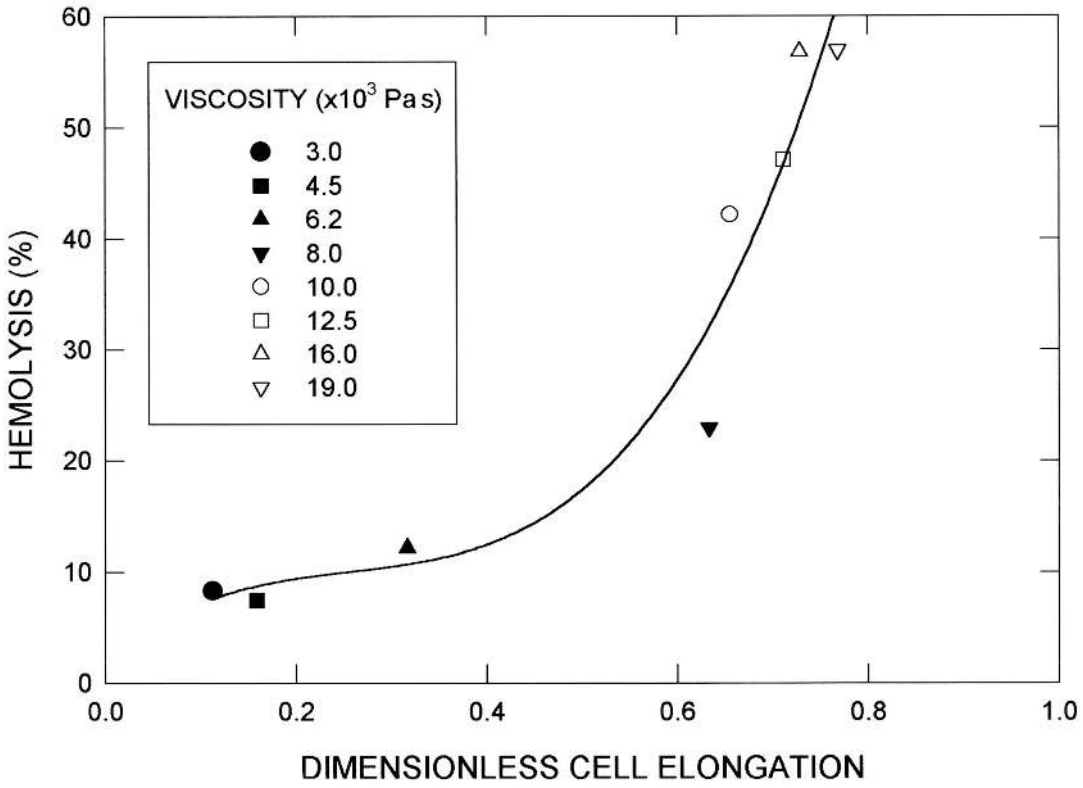

FIGURE 13. Increase in erythrocyte elongation and hemolysis at a constant laminar shear stress of 150 $N \cdot m^{-2}$ as viscosity of suspending medium increased from 3×10^{-3} to 2×10^{-2} Pa·s. Exposure time was 5 min in all cases. Cell elongation is a dimensionless parameter defined as (cell length - cell width)/(cell length + cell width). (Based on Williams.[126])

to decrease the elongation of human red cells suspended in a shear field,[102] presumably by producing some sort of cross-linking. Potentially, this methodology may improve survival of any fragile cell with a significant amount of cross-linkable protein in the membrane.[5] Also, additives that affect the fluidity of the plasma membrane, that is, the freedom of the bilayer membrane's constituents to move about, appear to affect the shear survivability of cells.[104] Increasing membrane fluidity correlates with increasing shear sensitivity.[104] Membrane fluidity increases with increasing temperature and can be manipulated in both directions with various additives.[104] Other additives may render the cell more susceptible to shear damage. Certain chemical lysins and some antigen-antibody reactions cause perforation of the cell membrane and leakage of intracellular material.[76] Cholesterol enrichment or depletion of the human erythrocyte membrane does not affect its viscosity.

Hemolysis of red cells is known to occur intravascularly *in vivo* as well as in various *in vitro* flow systems.[76] A number of studies have correlated hemolysis to flow in pumps, valves, heart-lung machines, blood dialyzers, and transfusion filters. In tubular flow, wall roughness of the scale of erythrocyte correlates with hemolysis.[76] Bubbles trapped in surface imperfections appear to aid lysis. In tubes, hemolysis correlates with the shear rate and the surface-to-volume ratio.[76] This type of lysis occurs at shear stress thresholds lower than the ones required to produce lysis in a fluid shear field. Wall contact-associated lysis has been observed to depend on the chemical nature of the wall material. Lysis may decline with time as surfaces become passivated by prolonged contact with plasma proteins.[76]

In capillaries of ~1 mm in diameter, an upper limit on the mean tube velocity of 6 $m \cdot s^{-1}$ has been suggested for capillaries with sharp-edged entrances, and blood with a viscosity of 4×10^{-3} Pa·s.[76] This corresponds to a Reynolds number of 1500 inside the capillary and an average wall shear rate of about 4800 s^{-1}. Velocities as high as 17 $m \cdot s^{-1}$ (i.e., a Reynolds number of ~4200) may be employed inside capillaries with carefully flared entrances.[76] As with other animal cells, erythrocytes subjected to bubbling are susceptible to bubble rupture-associated damage;[103] however, damage occurs also in surface aerated shake flasks, and the specific lysis rate increases with increasing speed of the shaker platform for the range of 100 to 400 rpm, as shown in Figure 14. The slight decline in lysis rate at 100 rpm (Figure 14) was associated with improved surface aeration relative to a static flask.[103]

In comparison with erythrocytes, the cytoplasm of leukocytes has markedly different rheological properties,[105] but the properties of leukocyte membrane are similar to those of the red cell membrane. Leukocytes adhering to vascular endothelium detach when the shear stress is between 26.5 and 106.0 $N \cdot m^{-2}$.[105] According to work cited by Prokop and Bajpai,[86] a shear stress level of 60 $N \cdot m^{-2}$ applied over 10 min should lyse about one-fourth of a leukocyte population. In another study, sublethal shear stresses of 10 and 20 $N \cdot m^{-2}$ applied over 10 min in a Couette viscometer affected the biochemical response of human T cells relative to unsheared controls.[106] Therefore, it seems, that cells *in vivo* in circulation are apparently more shear resistant than ones studied *in vitro*.

B. Adherent Cells

1. Cells on Stationary Surfaces

Quite low shear stress levels, for example, between 0.25 and 0.60 $N \cdot m^{-2}$ in laminar flow,[107] can interfere with the process of cell attachment to surfaces; however, once the cells are attached and spread out, they may tolerate higher stresses. Prevailing shear stress also affects how cells orient during attachment and spread on a surface. *In vitro* studies in a parallel plate laminar flow chamber (τ = 2.3 $N \cdot m^{-2}$) confirmed that surface adherent endothelial cells seeded under static conditions for 1 h, when exposed to flow, became oriented parallel to the flow axis and were more elongated than ones grown under static conditions.[108] When the static incubation period was lengthened (24 to 48 h) so that cells attained confluence, orientation was disparate and was not affected by subsequent flow. Morphological response of endothelial cells has been suggested as being indicative of local hydromechanical forces. A cell's adaptive response, for example, a reduced projected area relative to static conditions, reduces the fluid motion associated forces experienced by the cell.[108] The presence of suspended cells such as erythrocytes in the flowing fluid has been observed to affect the spread of attached endothelial cells. This effect is apparently due to collisions between suspended erythrocytes and the endothelial cells and also due to the viscosity enhancing effect of suspended cells. Laminar shear stress of the order of 0.5 to 10.0 $N \cdot m^{-2}$ may remove adherent cells from surfaces,[65] but even lower values (e.g., 0.1 to 1.0 $N \cdot m^{-2}$) are known to affect cellular morphology, permeability, and gene expression.[65]

Sublethal shear stress levels cause no obvious physical damage but may produce various biochemical and physiological responses.[106,109-112] Shear stress strongly stimulates endothelial cells to produce nitric oxide.[111] Other physiological responses have been reported. In studies with rat aortic endothelial cells anchored on the internal walls of glass capillaries, laminar shear stress was shown to affect the cytosolic pH because of preferential leakage of certain ions out of the cells into the buffer saline.[110] This reversible permeability enhancement occurred even at stress levels as low as 0.05 $N \cdot m^{-2}$ applied over short durations (~2 min). Similar effects were noted with human aortic endothelial cells but not with human skin fibroblasts or rat intes-

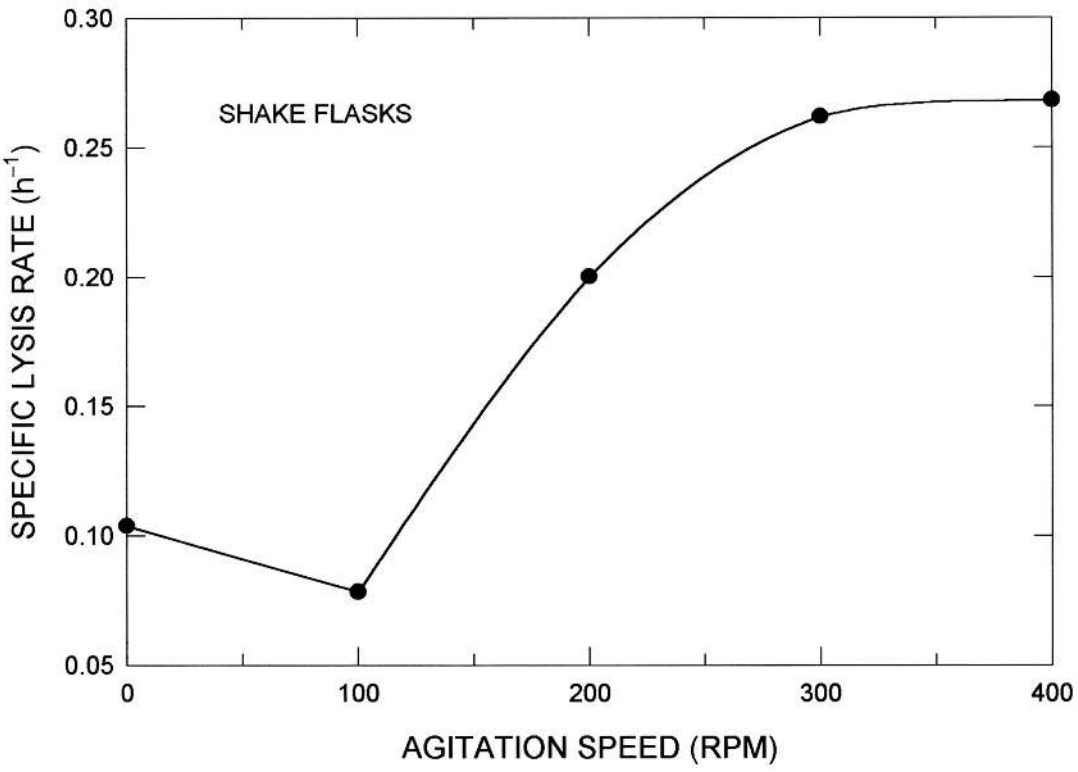

FIGURE 14. Effect of shaker platform agitation speed on specific lysis rate of suspended porcine erythrocytes in surface aerated shake flasks.[103]

tinal epithelial cells exposed to shear stress levels of up to 1.34 $N \cdot m^{-2}$.[110] With rat aortic cells, the flow induced cytosolic acidification could be maintained for at least 30 min at 1.34 $N \cdot m^{-2}$ shear stress level, but the cytosolic pH returned to unstressed values within about 15 min when the sustained shear stress was ≤0.027 $N \cdot m^{-2}$.[110]

In studies with anchorage-dependent cells attached to the flat glass walls of a rectangular flow channel, Shiragami and Unno[113] observed increased activity of lactate dehydrogenase (LDH) in cells that had been exposed to a steady state shear stress of 0.5 $N \cdot m^{-2}$ for 12 h; the activity was fourfold greater relative to controls. The LDH activity correlated with the transmission of energy from the fluid to the attached cells.[113]

In vivo hemodynamic forces have been implicated in various physiological and pathophysiological processes.[109] Atherosclerotic lesions in humans tend to develop in zones of flow separation[109] such as regions of arterial branching and sharp curvature. Arteries adapt to chronic changes in blood flow, increasing in circumference under high flow and narrowing under reduced flow.[109] Shear stress signals transmitted throughout the vascular cell via cytoskeletal and biochemical elements result in changes to structure, metabolism, and gene expression.[109]

2. Cells on Suspended Microcarriers

Microcarrier culture is the mainstay of processes for making viral vaccines and other cell culture-derived products.[1,2] Both stirred tank and airlift bioreactors[114] may be used for suspended microcarrier culture. Microcarrier-supported cells likely experience more severe hydrodynamic forces than do freely suspended cells. This is because in highly agitated or aerated systems, the length scale of fluid eddies can easily approach the dimensions of

microcarriers, resulting in high local relative velocities between the solid and the liquid phases.[3,47,115] In addition, the carriers have greater inertia than free cells; hence, collisions among microcarriers and between the impeller and microcarriers likely damage attached cells. Similarly, fluid eddy impact and shear stress forces on a high-inertia particle are greater than on freely suspended cells. Flow fields and local energy dissipation rates in spinner vessels have been characterized.[116] With regards to impeller- and hydrodynamics-associated damage to cells on microcarriers, the damage was hypothesized to originate predominantly in the trailing liquid vortex region near the impeller tips and the convergent flow zones above and below the impeller (Figure 15).

Resistance of a cell to rupture by impact (i.e., burst resistance) is a possible measure of the cell's survivability in the culture environment. Measurements of burst force are potentially also useful for the comparative assessment of cell strength and in establishing culture conditions that give rise to more robust cells. It may eventually be possible to correlate the sensitivity to shear of a cell to its resistance to mechanical rupture.[117] Burst strength may be directly relevant in microcarrier culture where impact-associated damage is likely; however, in view of the cytoskeleton-mediated pressure signal transmission[109,118] to internal parts of a cell and other biochemical effects of low-level shear stresses,[82,86,106,109,110,119] a more likely scenario is that the force required to cause impact-associated damage is far lower than the rupture threshold.[5] This issue notwithstanding, resistance to rupture of a mouse hybridoma grown in serum-containing continuous culture has been measured by squeezing single cells between flat surfaces of micromanipulator arms.[80] The bursting strength increased with cell size.[120] The bursting force correlated with the initial cell diameter as follows:

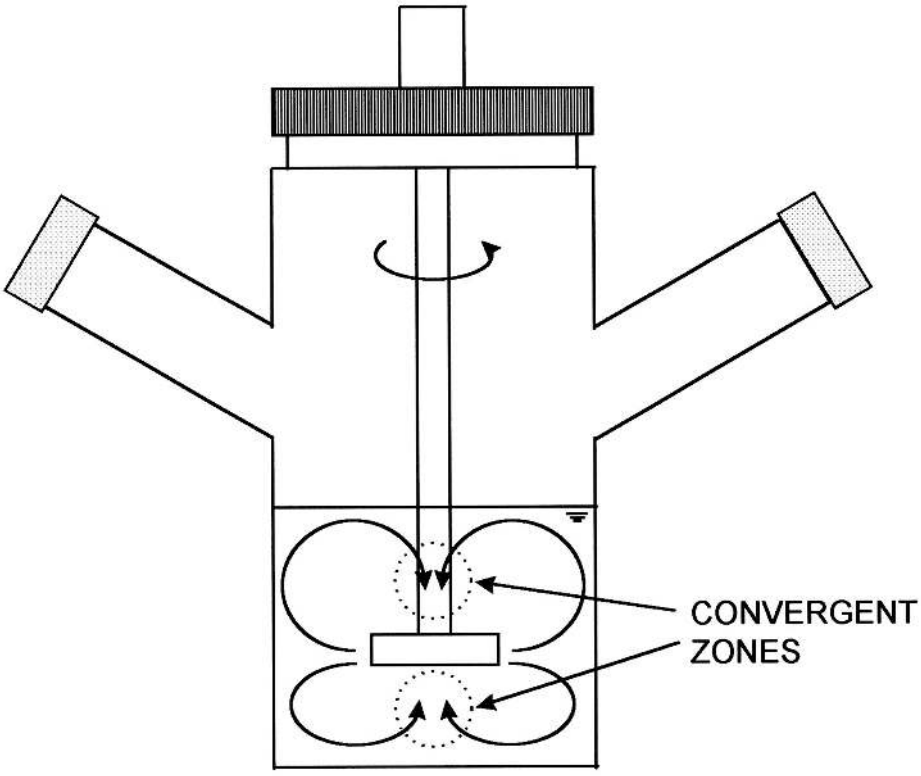

FIGURE 15. Convergent flow zones above and below the impeller of a spinner vessel where collisions among microcarriers could contribute to cell damage.

$$S = 0.2d_c - 0.1\times10^{-6} \quad (54)$$

where the intercept was not significantly different from zero.[80] The cell diameter ranged over ~(10-17) × 10^{-6} m. Other similar data[120] have been correlated[117] as follows:

$$S = 0.27d_c - 0.86\times10^{-6} \quad (55)$$

where the burst strength S is in newtons, and the hybridoma cell diameter, d_c, is in micrometers. The calculated bursting tension had a mean value of (1.8 ± 0.5) × 10^{-3} N·m^{-1}, which was essentially independent of cell size.[80] Because the bursting tension was size independent, the bursting pressure fell with increasing cell diameter. At (0.8 ± 0.3) × 10^{-3} N·m^{-1}, the calculated mean compressibility modulus of the cells was roughly independent of cell diameter.[80]

Sinskey et al.[121] advanced the concept of an integrated shear factor (ISF)—a measure of the strength of the shear field between the impeller and the spinner vessel walls—to correlate shear damage to mammalian cells. The ISF was defined as

$$\text{ISF} = \frac{2\pi N d_i}{d_T - d_i} \quad (56)$$

or, effectively, the laminar shear rate between the impeller tip and the walls. For a range of stirred vessels (0.25 to 2.0 L, 0.032 ≤ d_i (m) ≤ 0.085), cell damage occurred once the ISF value exceeded about 18 s^{-1} during culture of microcarrier-supported human fibroblasts.[50] The relative extent of cell growth declined sharply at the critical value of the integrated shear factor as shown in Figure 16. Damage could be correlated also with the impeller tip speed, but unlike the ISF the damaging value of the tip speed depended on the size of the culture vessel.[50] Despite its apparent success in correlating cell damage in some cases, the use of ISF is fundamentally unsound, especially when the aim is to scale up a bioreactor without affecting the survival behavior of cells. For example, in a standard stirred tank[60] with $d_T = 3\ d_i$, the damage controlling parameter ISF equals πN (see Eq. 56), that is, the damage depends solely on the rotational speed N of the impeller. If now the standard tank is scaled up to a geometrically similar larger vessel with a tank diameter that is twice that of the smaller reactor, and the two reactors are operated at the same rotational speed of impeller, the larger device will have twice the impeller tip speed relative to that of the smaller tank. If the smaller impeller was already at the upper acceptable tip speed limit, then a doubling of tip speed in the scaled up reactor is bound to damage cells on microcarriers. According to Eq. 56, for a damaging threshold ISF value of ~18 s^{-1} reported for microcarrier-supported fibroblasts,[50] an upper limit of acceptable rotational speed in a standard tank works out to ~6 rps *irrespective of scale*.

Relying on the earlier work of Nagata, Croughan et al.[50] developed the following relationship between a time averaged shear rate and the tank geometry:

$$\gamma_{\text{av·T}} = \frac{112.8 r_i^{1.8}\left(r_T^{0.2} - r_i^{0.2}\right)\left(r_c / r_i\right)^{1.8}}{r_T^2 - r_i^2} \quad (57)$$

where r_i and r_T are the impeller and the tank radii, respectively. The radius r_c of the formed vortex zone would need to be estimated using Nagata's expression:

$$\frac{r_c}{r_i} = \frac{\text{Re}_i}{1000 + 1.6\,\text{Re}_i} \quad (58)$$

The impeller Reynolds number in Eq. 58 is calculated as follows:

$$\text{Re}_i = \frac{N d_i^2 \rho_L}{\mu_L} \quad (59)$$

Equation 57 was developed for transitional and turbulent regimes ($\text{Re}_i \geq 10^3$) in unbaffled stirred

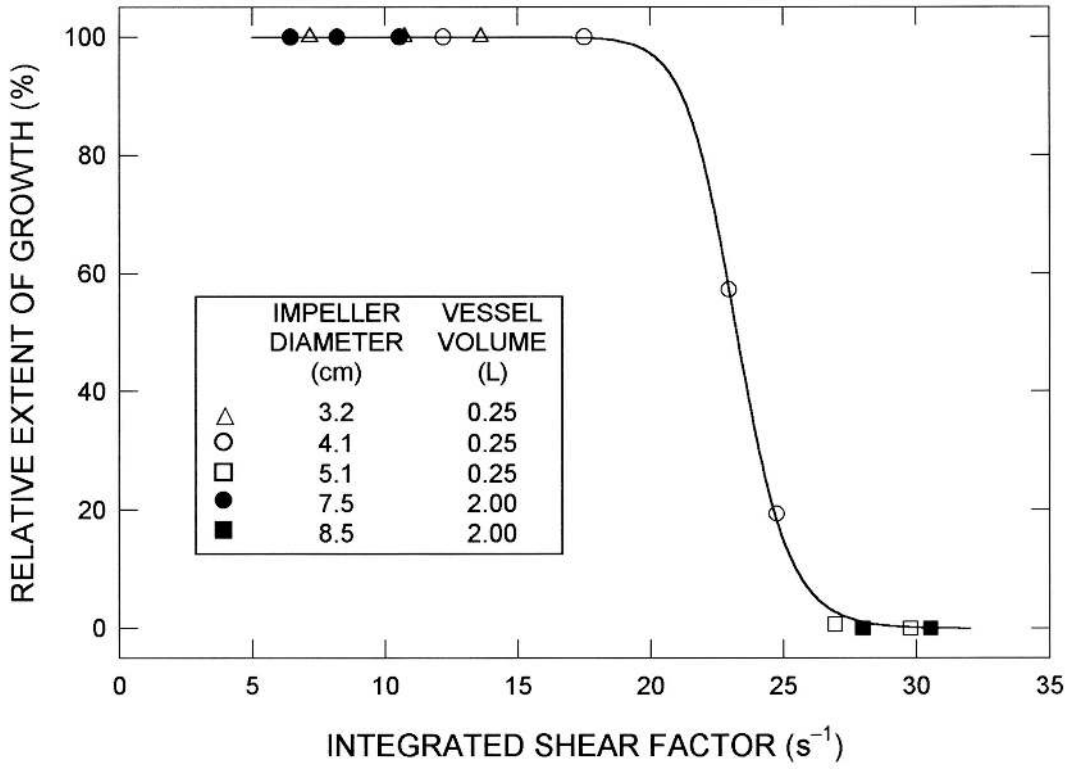

FIGURE 16. Relative extent of growth of human diploid fibroblasts on microcarriers as a function of the integrated shear factor in spinner vessels. All vessels had 5 g·L^{-1} microcarriers. (Based on Croughan et al.[50])

tanks.[50] Cells were damaged when the time-averaged shear rate exceeded about 2.5 s^{-1} in various stirred vessels containing human fibroblasts supported on microcarriers.[50] For chicken embryo fibroblasts, also on microcarriers, the damage threshold was 6 s^{-1} time-averaged shear rate.[50] Cell damage correlated also with the Kolmogoroff eddy length scale (ℓ): for human fibroblasts the cell damage occurred when the length scale declined to approximately below 125 μm (Figure 17), whereas for the chicken embryo cells damage was observed when the ℓ-value declined to below 100 μm.[50] The mean diameter of microcarriers was about 185 μm, or roughly similar to the length scale of the damage causing microeddies.

Analyzing data from several sources, Croughan et al.[50] further showed that the specific death rate correlated with the average energy dissipation rate per unit mass; thus,

$$k_d \propto E^m \qquad (60)$$

where m was 0.72, 0.76, and 0.82, respectively, for microcarrier-supported Vero cells, similarly supported human fibroblasts, and a freely suspended protozoan (cell diameter ~80 μm). For attaining a more homogeneous shear field in stirred culture vessels (i.e., for the minimum value of the maximum-to-average shear rate ratio), Croughan et al.[50] noted an optimal vessel geometry corresponding to $r_i/r_T = 0.74$..

In microcarrier culture, collisions between microcarriers and interactions between carriers and internals of a reactor are other possible causes of cell damage, particularly in stirred bioreactors.[3,57,92] Cherry and Papoutsakis[57,92,115] invoked "severity of collision" to account for at least some of the damage to cells in suspended microcarrier culture in stirred vessels. Severity of collision combined collision frequency and energy of the impact. Two collision severities were defined: a turbulent collision severity (TCS) for turbulence-associated particle-to-particle impacts, and an impeller

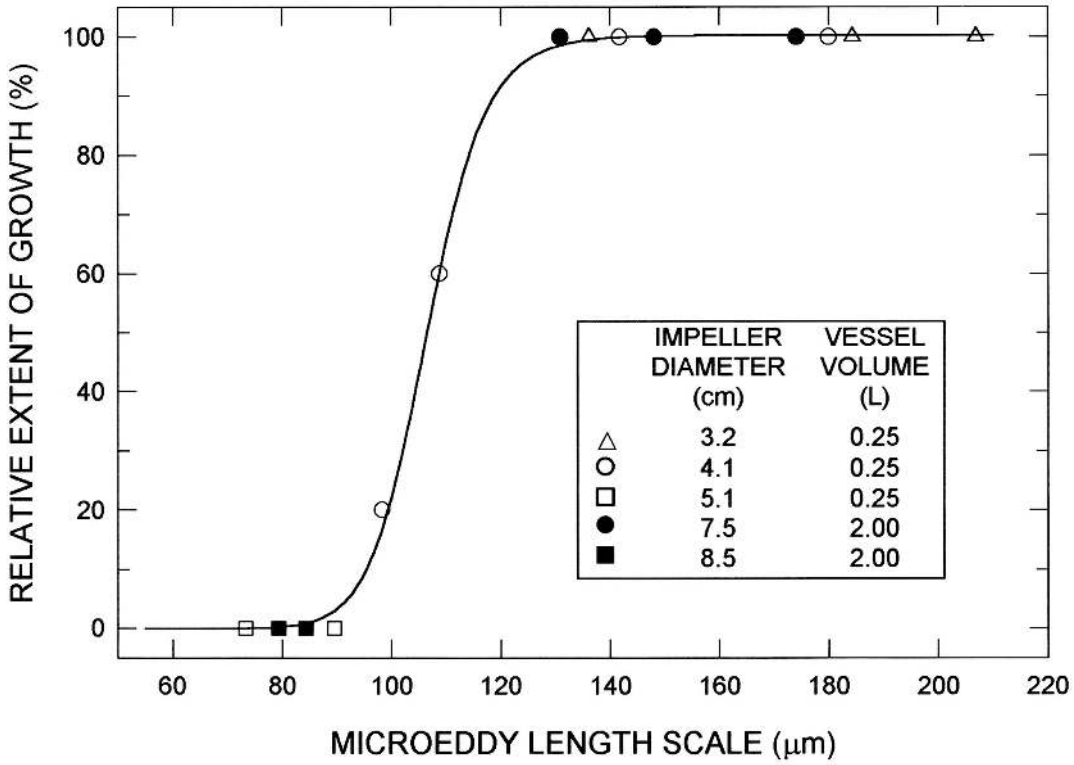

FIGURE 17. Relative extent of growth of human diploid fibroblasts on microcarriers as a function of the Kolmogoroff microscale of turbulence in spinner vessels. All cultures contained 5 g·L^{-1} microcarriers. (Based on Croughan et al.[50])

collision severity (ICS) for particle-to-impeller collisions; thus,

$$\mathrm{TCS} = \left(\frac{E\rho_L}{\mu_L}\right)^{3/2}\left(\frac{\pi^2\rho_S d_p^5 \varepsilon_S}{72}\right) \qquad (61)$$

and

$$\mathrm{ICS} = \frac{9\pi^4\rho_S n_B N^3 d_i^4 d_p^4}{512 V_L} \qquad (62)$$

where E is the energy dissipation rate per unit liquid mass, ρ_S and d_p are the density and diameter of the microcarriers, ε_S is the volume fraction of the carriers, n_B is the number of impeller blades, N and d_i are the impeller rotational speed and diameter, and V_L is the volume of the liquid in the vessel. Improved cell growth was observed with smaller microcarriers, as predicted by Eq. 61 and Eq. 62. The specific cell death rate increased with increasing values of TCS and ICS[57,92] however, the influence of hydrodynamic forces on culture performance correlated also in terms of the ratio of Kolmogoroff eddy scale to bead diameter: the specific death rate declined as ℓ/d_p increased. As culture viscosity was raised, damage to cells declined in conformance with Eq. 61 and in agreement with interpretations based on the ℓ/d_p ratio.[57]

Unlike in stirred tanks (Figure 15), animal cell microcarriers suspended in airlift bioreactors under typical operating conditions do not significantly interact with each other or with the walls of the vessel[122] instead, the microcarrier particles follow the laminar streamlines of the fluid.[122] Consequently, in airlift reactors at least, the effects of particle-particle or particle-wall collisions on monolayers of cells may be disregarded. Observations of Ganzeveld et al.[122] spanned microcarrier loadings of up to 30 kg·m^{-3}, with carriers of 150 to

300 mm diameter, and 1030 to 1050 $kg \cdot m^{-3}$ density. The observations covered a power input value of up to 33 $W \cdot m^{-3}$, which is about the upper limit for cell culture in pneumatically agitated bioreactors. These results applied to a split-cylinder airlift bioreactor with an aspect ratio of 7.6, which would not normally be exceeded in large-scale cell culture systems. As an additional design constraint, the Reynolds number in the riser and the downcomer should not exceed about 3000, or the flow will be more chaotic.[122]

In microcarrier culture, during inoculation, the round cells must first attach to microcarriers before spreading on the solid surface (Figure 18); hence, mechanics of cell attachment and how they are affected by the hydrodynamic conditions are relevant. Similarly, during proliferation, bead-to-bead transfer of cells[123] may also require a level of turbulence that is not so high as to hinder the reattachment process, yet not so low that bead-to-bead encounters are few. Attachment, detachment, and spread of cells are important in other situations also. For example, healing of vascular injury depends on growth and spread of endothelial cells. Attachment and proliferation of adherent cells is affected even by low levels of shear stress. Numerical analysis of forces exerted by laminar flow on anchorage-dependent cells attached to flat surfaces suggests that shear stress between 0.25 and 0.6 $N \cdot m^{-2}$ is sufficient to detach round cells, but much higher values are needed to dislodge spread out cells.[107] In one study, flow-induced detachment of mouse fibroblasts L929 from a glass surface required a stress (detachment force per unit cell adhesive area) of 530 to 750 Pa.[124] The detachment stress depended on the length of the static seeding period prior to the detachment experiments. Sensitivity of the microcarrier-attached cells to hydrodynamic forces depends also on the cell type.[125] Microcarrier-anchored Vero cells are apparently more sensitive than CHO-K1 and BHK-21 cell lines.[125]

Typically, the shear rate values in airlift bioreactors range over 250 to 4,000 s^{-1} for operational conditions that are relevant to animal cell culture.[12] These shear rates are substantially lower than the ~10^5 s^{-1} that would be needed to damage cells if a 100 $N \cdot m^{-2}$ shear stress value[11,85] is taken as the threshold of mechanical damage. However, based on the shear stress data of Olivier and Truskey,[107] during the process of attachment of cells to microcarriers, shear rate levels of 250 to 600 s^{-1} may well be detrimental. Thus, during initial attachment of cells, the reactor will need to be operated at a reduced aeration rate—a practice that is well established through empirical experience, but understood only intuitively.[12]

Under conditions typical of microcarrier culture in airlift bioreactors, the specific energy dissipation rates are different in different zones of the vessel. The specific energy dissipation rates increase in the following order: downcomer < riser < bottom, for any fixed value of the aeration rate.[12] In addition to the value of the specific energy dissipation rate in various zones, the geometry of the flow path appears to also determine whether damage occurs and its magnitude. For example, flow over or under sharp-edges can damage cells,[76,127] especially larger ones and those anchored on microcarriers. Such edges occur at entrances and exits of downcomers and risers in airlift bioreactors, but can be hydrodynamically smoothed to prevent flow separation, turbulence, and cell damage (Figure 19).

The shear rates in all zones in an airlift device decline with increasing loading of microcarriers; however, the prevailing shear rates are not particularly sensitive to the density or the diameter of microcarriers within the ranges that are relevant to anchorage-dependent cell culture. In one case, typical shear rates ranged over 250 to 4000 s^{-1} in microcarrier-containing systems, but much higher values, up to 12,000 s^{-1} could occur in solids-free media.[12] These values compare favorably with shear rates of ~10^5 s^{-1} that have been reported as the threshold of damage to cells. Cells in airlift bioreactors would experience a substantial increase in the riser shear rate only when the fluid eddy length-to-microcarrier diameter ratio declines to ~1.[12]

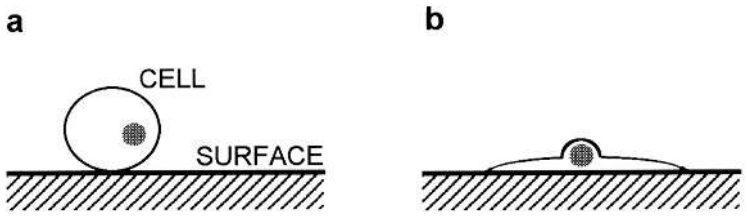

FIGURE 18. A spherical cell encountering a surface first attaches or adsorbs (a) and then spreads out over the surface (b) because the cell-surface interfacial tension exceeds the membrane tension.

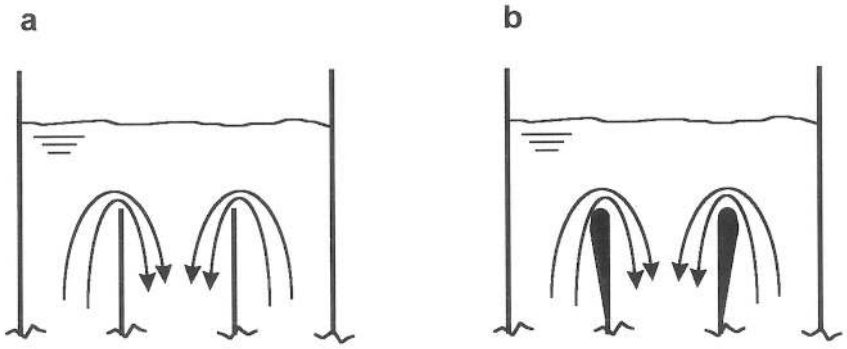

FIGURE 19. (a) Flow over or under a sharp edge as in the entrance to the downcomer of an airlift bioreactor may damage cells. (b) Hydrodynamically smoothed flow path prevents flow separation and reduces damage to large cells and cells anchored on microcarriers.

Fluid eddies a little smaller than the dimensions of microcarriers may cause the latter to rotate. According to Cherry and Papoutsakis,[115] the maximum and average shear rates on a rotating microcarrier bead may be calculated using the equations:

$$\tau_{av} = 0.5\mu_L\gamma_i \quad (63)$$

$$\tau_{max} = 3\mu_L\gamma_i \quad (64)$$

where γ_i is the shear rate associated with turbulent microeddies at a given power input in the absence of microcarriers. The γ_i value is calculated using Eq. 34 and Eq. 35. For a given specific power input, the shear stress increases with increasing viscosity of the suspending fluid, as shown in Figure 20.

C. Shear Effects on the Cell Cycle

From one division to the next, a cell goes through a sequence of recognizable phases that involve intracellular reorganization in preparation for division. The phases between two consecutive division events constitute the cell cycle. In classic interpretation of the mammalian cell cycle (Figure 21), the different phases are as follows: the G_0 gap phase 0, in which the cell may survive for extended periods without division and outside the normal cycle; the G_1 gap phase 1; the S synthesis phase, in which cytoplasmic components are synthesized and DNA is replicated; the G_2 gap phase 2; and the mitotic (or meiosic) M phase, the end of which is marked by cell division. Cell cycles of all eukaryotes are generally similar but markedly different from the bacterial cell cycle. The cell cycle is subject to various kinds of environmental influences, including the availability of nutrients and growth factors, temperature, and also hydrodynamics factors. Cells in culture are generally at different stages of the cell cycle, unless the cycles are synchronized by external stimuli. Certain phases of the cell cycle may be more conducive to producing certain proteins and chemical additives may be used to arrest cells, at least temporarily, in a given phase. The speed of the cycle may also be modulated.

Significant direct and indirect evidence supports that hydrodynamic forces affect the cycle of animal cells. Rate of DNA synthesis and the relative proportions of the cells in the various stages of the cell cycle are influenced by agitation and gas sparging, as observed by Lakhotia et al.[128] In intensely agitated cultures, the fraction of the cells in the S phase was up to 45% greater relative to control cultures, and there were up to 50% fewer cells in the G_1 phase.[128] Once the external stress was removed, the culture returned to the normal state after an stabilization period. In another case, the fraction of cells in the various phases was altered on passage through a turbulent capillary[98] because of preferential loss of S and G_2 cells that are larger relative to cells in other phases of the cell cycle. Also noteworthy here is the hydrodynamics-induced apoptosis[97,98] (see Section III.A.1), as apoptosis is regulated by some of the same mechanisms that control the cell cycle. How exactly an external mechanical force influences the cell cycle is not known, but possible modes of action include cytoskeleton-mediated stress transmission (see Section III.B.1) and the biochemical responses linked to cell surface mechanoreceptors.

IV. CONCLUDING REMARKS

Animal cells are affected and damaged by hydrodynamic stresses both in laminar and turbulent flows even in the absence of gas bubbles. Cells vary a great deal in susceptibility to shear damage. Even in well-defined laminar flow, the damaging threshold of shear stress may vary by more than 10-fold for different cells. Several kinds of damaging forces are typically encountered simultaneously in a given process device. For a given cell, the shear response is determined by the intensity, duration, and type of the force. Survival dynamics of the cell are influenced by how often the damaging forces

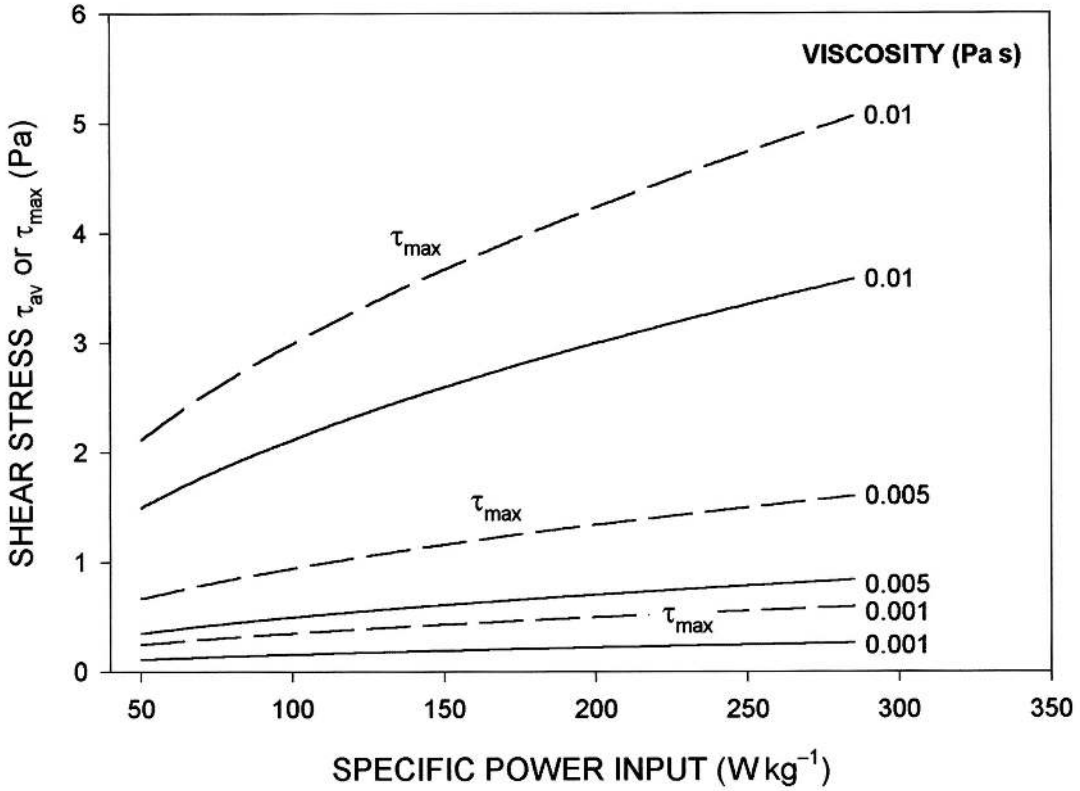

FIGURE 20. Effects of culture viscosity and specific power input on mean and maximum shear stress values on the surface of suspended microcarriers. Shear stress was calculated according to Eq. 63 and Eq. 64.

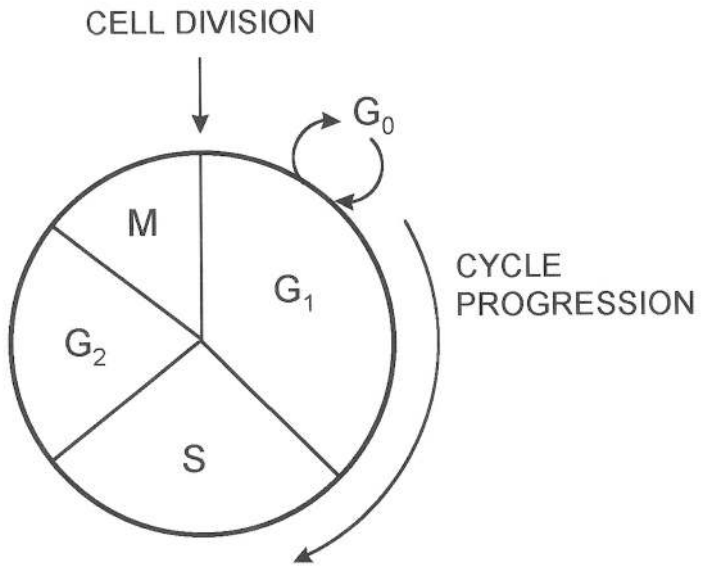

FIGURE 21. The mammalian cell cycle. A cell in G_1 phase may go out of the normal cycle and into a resting G_0 phase.

are encountered, that is, by the frequency of encounter, during the processing period. Turbulent shear stress is generally more damaging than laminar shear stress of the same magnitude. For some cells, the sensitivity to damaging force appears to vary with the stage of growth, but for others no such effect seems to occur. Under given conditions, the rate of cell inactivation or damage is typically first order in cell number. Compared with human cells, murine lines appear to be generally less tolerant of shear stresses.

V. NOMENCLATURE

ΔA_B	Increase in surface area at burst (m^2)
A_d	Cross-sectional area of the downcomer (m^2)
A_o	Original surface area of cell (m^2)
A_r	Cross-sectional area of the riser (m^2)
a	Parameter in Eq. (2) (–)
BHK	Baby hamster kidney cells
BSA	Bovine serum albumin
C	Constant in Eq. (31) (–)
C_f	Fanning friction factor (–)
CHO	Chinese hamster ovary cells
d	Diameter or hydraulic diameter (m)
d_B	Bubble diameter (m)
d_c	Cell diameter (μm)
d_f	Deformation of drop or cell (–)
d_{fb}	Deformation at burst (–)
d_i	Impeller diameter (m)
d_p	Microcarrier or particle diameter (m)
d_{pm}	Mean value of cell or particle diameter (m)
d_{ps}	Standard deviation of d_{pm} (m)
d_T	Tank or column diameter (m)
E	Energy dissipation rate per unit mass ($W \cdot kg^{-1}$)
FBS	Fetal bovine serum
g	Gravitational acceleration ($m \cdot s^{-2}$)
h	Channel height (m)
h_b	Height of impeller blade (m)
h_D	Height of gas-liquid dispersion (m)
ICS	Impeller collision severity defined by Eq. 62 ($kg \cdot m^{-2}s^{-3}$)
ISF	Integrated shear factor defined by Eq. 56 (s^{-1})
K	Consistency index ($Pa \cdot s^n$)
k	Parameter in Eq. (2) (m^{-1})
k_d	Death rate constant (s^{-1})
k_i	Constant in Eq. (19) (–)
L	Length of tube or channel (m)
LDH	Lactate dehydrogenase
ℓ	Mean microeddy length (m)
ℓ_e	Length of the energy-containing eddy (m)
m	General exponent (–)
N	Rotational speed (s^{-1}) or cell concentration (m^{-3})
n	Flow behavior index (–)
n_B	Number of impeller blades (–)
ΔP	Pressure drop (Pa)
P_B	Expected fraction of burst cells (%)
Po	Power number
P_T	Total power input (W)
P_τ	Percentage cell rupture at shear stress τ (%)
p	Normalized cell diameter defined by Eq. 52 (–)
q	Normalized burst tension ($N \cdot m^{-1}$)
Re_i	Impeller Reynolds number defined by Eq. 59 (–)
r	Radial distance (m)
r_c	Radius of the vortex zone defined by Eq. 58 (m)
r_i	Impeller radius (m)
r_T	Tank radius (m)
S	Burst strength (N)
Ta	Taylor number (-)
TCS	Turbulent collision severity for particle-to-particle collisions ($kg \cdot m^{-2}s^{-3}$)
U_B	Bubble rise velocity ($m \cdot s^{-1}$)
U_G	Superficial gas velocity ($m \cdot s^{-1}$)
U_{Gr}	Superficial gas velocity in riser ($m \cdot s^{-1}$)
U_L	Average liquid velocity ($m \cdot s^{-1}$)
U_T	Peripheral or tip speed ($m \cdot s^{-1}$)
u	Mean velocity of the microeddies ($m \cdot s^{-1}$)
u_l	Local velocity ($m \cdot s^{-1}$)
u_{max}	Maximum or centerline velocity ($m \cdot s^{-1}$)
u_o	Jet velocity at orifice ($m \cdot s^{-1}$)
V_D	Volume of gas-liquid dispersion (m^3)
V_L	Volume of liquid (m^3)

V_s	Effective energy dissipation volume or the volume swept by the impeller (m^3)
W	Width of the impeller blade (m)
w	Viscometer gap width (m)
x	Distance along x axis (m)
y	Distance along y axis (m)
Z	Parameter defined by Eq. 50 (–)

A. Greek Symbols

β	Parameter in Eq. 30 (–)
γ	Shear rate (s^{-1})
γ_{av}	Average shear rate (s^{-1})
$\gamma_{av,T}$	Time-averaged shear rate (s^{-1})
γ_I	Shear rate in the region around the impeller (s^{-1})
γ_i	Isotropic turbulence shear rate defined by Eq. 34 (s^{-1})
γ_{max}	Time averaged maximum shear rate (s^{-1})
γ_w	Wall shear rate (s^{-1})
ε_S	Volume fraction of microcarriers or solids (–)
η	Constant in Eq. 33 (–)
θ	Parameter defined by Eq. 48 (–)
μ_{ap}	Effective or apparent viscosity (Pa·s)
μ_d	Viscosity of the drop phase (Pa·s)
μ_L	Viscosity of liquid (Pa·s)
π	Pi (-)
ρ_L	Density of liquid ($kg \cdot m^{-3}$)
ρ_S	Density of microcarriers or solid ($kg \cdot m^{-3}$)
σ	Interfacial tension or membrane tension ($N \cdot m^{-1}$)
σ_B	Membrane tension at cell burst ($N \cdot m^{-1}$)
σ_{Bm}	Mean value of σ_B ($N \cdot m^{-1}$)
σ_{Bs}	Standard deviation of σ_{Bm} ($N \cdot m^{-1}$)
τ	Shear stress ($N \cdot m^{-2}$)
τ_{av}	Average value of Kolmogoroff shear stress on microcarrier ($N \cdot m^{-2}$)
τ_{max}	Maximum value of Kolmogoroff shear stress on microcarrier ($N \cdot m^{-2}$)
$\tau_{max\ J}$	Maximum shear stress in a submerged free jet ($N \cdot m^{-2}$)
τ_w	Wall shear stress ($N \cdot m^{-2}$)
φ	Parameter defined by Eq. 44 (–)

REFERENCES

1. Lubiniecki, A.S., Ed., 1990. *Large-Scale Mammalian Cell Culture Technology*. Dekker, New York.
2. Spier, R.E., Ed., 2000. *Encyclopedia of Cell Technology*, John Wiley, New York.
3. Papoutsakis, E.T., 1991. Fluid-mechanical damage of animal cells in bioreactors. *Trends Biotechnol.* **9**, 427–437.
4. Papoutsakis, E.T., 1991. Media additives for protecting freely suspended animal cells against agitation and aeration damage. *Trends Biotechnol.* **9**, 316–324.
5. Chisti, Y., 1999. Shear sensitivity. In: Flickinger, M.C., Drew, S.W. (Eds.), in *Encyclopedia of Bioprocess Technology: Fermentation, Biocatalysis, and Bioseparation*. Vol. 5, John Wiley, New York, pp. 2379–2406.
6. Chisti, Y., 2000. Animal-cell damage in sparged bioreactors. *Trends Biotechnol*. **18**, 420–432.
7. Chattopadhyay, D., Garcia-Briones, M., Venkat, R., and Chalmers, J.J., 1997. Hydrodynamic properties in bioreactors. In: Hauser, H., Wagner, R. (Eds.), *Mammalian Cell Biotechnology in Protein Production*. Walter de Gruyter & Co., Berlin, pp. 319–343.
8. Chalmers, J.J., 1998. Gas bubbles and their influence on microorganisms. *Appl. Mech. Rev.* **51**, 113–120.
9. Hua, J., Erickson, L.E., Yiin, T.-Y., and Glasgow, L.A., 1993. Review of the effects of shear and interfacial phenomena on cell viability. *Crit. Rev. Biotechnol.* **13**, 305–328.
10. Augenstein, D.C., Sinskey, A.J., and Wang, D.I.C., 1971. Effect of shear on the death of two strains of mammalian tissue cells. *Biotechnol. Bioeng.* **13**, 409–418.
11. Born, C., Zhang, Z., Al-Rubeai, M., and Thomas, C.R., 1992. Estimation of disruption of animal cells by laminar shear stress. *Biotechnol. Bioeng.* **40**, 1004–1010.
12. Grima, E., Chisti, Y., and Moo-Young, M., 1997. Characterization of shear rates in airlift bioreactors for animal cell culture. *J. Biotechnol.* **54**, 195–210.
13. McQueen, A., Meilhoc, E., and Bailey, J.E., 1987. Flow effects on the viability and lysis of sus-

pended mammalian cells. *Biotechnol. Lett.* **9**, 831–836.

14. Ludwig, A., Kretzmer, G., and Schügerl, K., 1992. Determination of a "critical shear stress level" applied to adherent mammalian cells. *Enzyme Microb. Technol*. **14**, 209–213.

15. Shiragami, N., 1994. Development of a new method for testing strength of cells against fluid shear stress. *Bioprocess Eng*. **10**, 47–51.

16. Thomas, C.R., 1990. Problems of shear in biotechnology. In: Winkler, M.R. (Ed.), *Chemical Engineering Problems in Biotechnology*. Elsevier, London, pp. 23–93.

17. Chisti, Y., 1989. *Airlift Bioreactors.* Elsevier, London.

18. Chisti, Y., 1998. Pneumatically agitated bioreactors in industrial and environmental bioprocessing: Hydrodynamics, hydraulics and transport phenomena. *Appl. Mech. Rev.* **51**, 33–112.

19. Chisti, Y. and Moo-Young, M., 1989. On the calculation of shear rate and apparent viscosity in airlift and bubble column bioreactors. *Biotechnol. Bioeng*. **34**, 1391–1392.

20. Lutkemeyer, D., Ameskamp, N., Tebbe, H., Wittler, J., and Lehmann, J., 1999. Estimation of cell damage in bench- and pilot-scale affinity expanded-bed chromatography for the purification of monoclonal antibodies. *Biotechnol. Bioeng*. **65**, 114–119.

21. Chisti, Y., 1998. Strategies in downstream processing. In: Subramanian, G. (Ed.), *Bioseparation and Bioprocessing: A Handbook.* Vol. 2, Wiley-VCH, New York, pp. 3–30.

22. Vogel, J.H. and Kroner, K.-H., 1999. Controlled shear filtration: a novel technique for animal cell separation. *Biotechnol. Bioeng.* **63**, 663–674.

23. Arathoon, W.R. and Birch, J.R., 1986. Large-scale cell culture in biotechnology. *Science* **232**, 1390–1395.

24. Birch, J.R., Lambert, K., Thompson, P.W., Kenney, A.C., and Wood, L.A., 1987. Antibody production with airlift fermentors. In: Lydersen, B.K. (Ed.), *Large Scale Cell Culture Technology.* Hanser Publishers, New York, pp. 1–20.

25. Emery, A.N., Lavery, M., Williams, B., and Handa, A., 1987. Large-scale hybridoma culture. In: Webb, C., Mavituna, F. (Eds.), *Plant and Animal Cells: Process Possibilities*. Ellis Horwood, Chichester, pp. 137–146.

26. Handa, A., Emery, A.N., and Spier, R.E., 1987. On the evaluation of gas-liquid interfacial effects on hybridoma viability in bubble column bioreactors. *Devel. Biol. Stand.* **66**, 241–253.

27. Handa-Corrigan, A., Emery, A.N., and Spier, R.E., 1989. Effect of gas-liquid interfaces on the growth of suspended mammalian cells: mechanisms of cell damage by bubbles. *Enzyme Microb. Technol*. **11**, 230–235.

28. Jöbses, I., Martens, D., and Tramper, J., 1991. Lethal events during gas sparging in animal cell culture. *Biotechnol. Bioeng*. **37**, 484–490.

29 Martens, D.E., de Gooijer, C.D., Beuvery, E.C., and Tramper, J., 1992. Effect of serum concentration on hybridoma viable cell density and production of monoclonal antibodies in CSTRs and on shear sensitivity in air-lift loop reactors. *Biotechnol. Bioeng*. **39**, 891–897.

30. Tramper, J., Joustra, D., and Vlak, J.M., 1987. Bioreactor design for growth of shear-sensitive insect cells. In: Webb, C., Mavituna, F. (Eds.), *Plant and Animal Cells: Process Possibilities*. Ellis Horwood, Chichester, pp. 125–136.

31. Tramper, J., Smit, D., Straatman, J., and Vlak, J.M., 1987. Bubble column design for growth of fragile insect cells. *Bioprocess Eng.* **2**, 37–41.

32. Shi, L.K., Riba, J.P., and Angelino, H., 1990. Estimation of effective shear rate for aerated non-Newtonian liquids in airlift bioreactor. *Chem. Eng. Commun.* **89**, 25–35.

33. Nishikawa, M., Kato, H., and Hashimoto, K., 1977. Heat transfer in aerated tower filled with non-Newtonian liquid. *Ind. Eng. Chem. Process Des. Develop.* **16**, 133–137.

34. Henzler, H.J., 1980. Begasen höherviskoser Flüssigkeiten. *Chem. -Ing. -Techn.* **52**, S 643–652.

35. Henzler, H.J. and Kauling, J., 1985. Scale-up of mass transfer in highly viscous liquids. Presented at the 5th European Conference on Mixing, Würzberg, Germany, paper 30, BHRA, Cranfield, pp. 303–312.

36. Schumpe, A. and Deckwer, W.-D., 1987. Viscous media in tower bioreactors: Hydrodynamic characteristics and mass transfer properties. *Bioprocess Eng*. **2**, 79–94.

37. Kawase, Y. and Moo-Young, M., 1986. Influence of non-Newtonian flow behaviour on mass transfer in bubble columns with and without draft tubes. *Chem. Eng. Commun.* **40**, 67–83.

38. Kawase, Y. and Kumagai, T., 1991. Apparent viscosity for non-Newtonian fermentation media in bioreactors. *Bioprocess Eng.* **7**, 25–28.

39. Al-Masry, W.A., 1999. Effect of scale-up on average shear rates for aerated non-Newtonian liquids in external loop airlift reactors. *Biotechnol. Bioeng.* **62**, 494–498.

40. Hoffmann, J., Buescher, K., and Hempel, D.C., 1995. Determination of maximum shear-stress in stirred vessels. (In German.) *Chem. -Ing. -Techn.* **67**, 210–214.

41. Robertson, B. and Ulbrecht, J.J., 1987. Measurement of shear rate on an agitator in a fermentation broth. In: Ho, C.S., Oldshue, J.Y. (Eds.), *Biotechnology Processes: Scale-Up and Mixing*. American Institute of Chemical Engineers, New York, pp. 31–35.

42. Chisti, Y., Halard, B. and Moo-Young, M., 1988. Liquid circulation in airlift reactors. *Chem. Eng. Sci.* **43**, 451–457.

43. Hülscher, M., Pauli, J., and Onken, U., 1990. Influence of protein concentration on mechanical cell damage and fluid dynamics in airlift reactors for mammalian cell culture. *Food Biotechnol.* **4(1)**, 157–166.

44. Okada, K., Shibano, S., and Akagi, Y., 1993. Turbulent properties in bubble-flow region in external-loop airlift bubble column. *J. Chem. Eng. Jpn* **26**, 637–643.

45. Lübbert, A. and Larson, B., 1990. Detailed investigations of the multiphase flow in airlift tower loop reactors. *Chem. Eng. Sci.* **45**, 3047–3053.

46. Lübbert, A., Larson, B., Wan, L.W., and Bröring, S., 1990. Local mixing behaviour of airlift multiphase chemical reactors. I. *Chem. E. Symp. Ser.* **121**, 203–213.

47. Chisti, Y., 1993. Animal cell culture in stirred bioreactors: observations on scale-up. *Bioprocess Eng.* **9**, 191–196.

48. Elias, C.B., Desai, R.B., Patole, M.S., Joshi, J.B., and Mashelkar, R.A., 1995. Turbulent shear stress–effect on mammalian cell culture and measurement using laser doppler anemometer. *Chem. Eng. Sci.* **50**, 2431–2440.

49. Michaels, J.D., Petersen, J.F., McIntire, L.V., and Papoutsakis, E.T., 1991. Protection mechanisms of freely suspended animal cells (CRL 8018) from fluid-mechanical injury. Viscometric and bioreactor studies using serum, Pluronic F68 and polyethylene glycol. *Biotechnol. Bioeng.* **38**, 169–180.

50. Croughan, M.S., Hamel, J.-F., and Wang, D.I.C., 1987. Hydrodynamic effects on animal cells grown in microcarrier cultures. *Biotechnol. Bioeng.* **29**, 130–141.

51. Croughan, M.S., Sayre, E.S., and Wang, D.I.C., 1989. Viscous reduction of turbulent damage in animal cell culture. *Biotechnol. Bioeng.* **33**, 862–872.

52. Lavery, M. and Nienow, A.W., 1987. Oxygen transfer in animal cell culture medium. *Biotechnol. Bioeng.* **30**, 368–373.

53. Oh, S.K.W., Nienow, A.W., Al-Rubeai, M., nd Emery, A.N., 1989. The effects of agitation intensity with and without continuous sparging on the growth and antibody production of hybridoma cells. *J. Biotechnol.* **12**, 45–62.

54. Oh, S.K.W., Nienow, A.W., Al-Rubeai, M., and Emery, A.N., 1992. Further studies of the culture of mouse hybridomas in an agitated bioreactor with and without continuous sparging. *J. Biotechnol.* **22**, 245–270.

55. Smith, C.G. and Greenfield, P.F., 1992. Mechanical agitation of hybridoma suspension cultures: metabolic effects of serum, Pluronic F68, and albumin supplements. *Biotechnol. Bioeng.* **40**, 1045–1055.

56. van der Pol, L. and Tramper, J., 1998. Shear sensitivity of animal cells from a culture-medium perspective. *Trends Biotechnol.* **16**, 323–328.

57. Cherry, R.S. and Papoutsakis, E.T., 1989. Growth and death rates of bovine embryonic kidney cells in turbulent microcarrier bioreactors. *Bioprocess Eng.* **4**, 81–89.

58. Bowen, R., 1986. Unraveling the mysteries of shear-sensitive mixing systems. *Chem. Eng.* June 9, 55–63.

59. Calderbank, P.H. and Moo-Young, M.B., 1959. The prediction of power consumption in the agitation of non-Newtonian fluids. *Trans. I. Chem. E.* **37**, 26–33.

60. Chisti, Y. and Moo-Young, M., 1999. Fermentation technology, bioprocessing, scale-up and manufacture. In: Moses, V., Cape, R.E., Springham, D.G. (Eds.), *Biotechnology: The Science and the Business*. 2nd ed., Harwood Academic Publishers, New York, pp. 177–222.

61. Candia, J.-L.F. and Deckwer, W.-D., 1999. Xanthan gum. In: Flickinger, M.C., Drew, S.W. (Eds.), *Encyclopedia of Bioprocess Technology: Fermentation, Biocatalysis, and Bioseparation.* Vol. 5, John Wiley, New York, pp. 2695–2711.

62. Jan, D.C.-H., Emery, A.N. and Al-Rubeai, M., 1993. Use of a spin-filter can reduce disruption of hybridoma cells in a bioreactor. *Biotechnol. Techniques* **7**, 351–356.

63. LaPorte, T.L., Shevitz, J., Kim, Y., and Wang, S.S., 1996. Long term shear effects on a hybridoma cell line by dynamic perfusion devices. *Bioprocess Eng.* **15**, 1–7.

64. Chisti, Y., 1992. Assure bioreactor sterility. *Chem. Eng. Progress* **88**(*9*), 80–85.

65. Aunins, J.G. and Henzler, H.-J., 1993. Aeration in cell culture bioreactors. In: Rehm, H.-J., Reed, G. (Eds.), *Biotechnology*. Vol. 3, 2nd ed., VCH, Weinheim, pp. 219–281.

66. Chisti, Y., 1999. Mass transfer. In: Flickinger, M.C., Drew, S.W. (Eds.), *Encyclopedia of Bioprocess Technology: Fermentation, Biocatalysis, and Bioseparation.* Vol. 3, John Wiley, New York, pp. 1607–1640.

67. Baldyga, J., Bourne, J.R., and Zimmerman, B., 1994. Investigation of mixing in jet reactors using fast, competitive-consecutive reactions. *Chem. Eng. Sci.* **49**, 1937–1946.

68. Baldyga, J., Bourne, J.R., and Gholap, R.V., 1995. The influence of viscosity on mixing in jet reactors. *Chem. Eng. Sci*. **50**, 1877–1880.

69. Nienow, A.W., 1998. Hydrodynamics of stirred bioreactors. *Appl. Mech. Rev*. **51**, 3–32.

70. Michaels, J.D., Mallik, A.K., and Papoutsakis, E.T., 1996. Sparging and agitation-induced injury of cultured animal cells: do cell-to-bubble interactions in the bulk liquid injure cells? *Biotechnol. Bioeng*. **51**, 399–409.

71. Meier, S.J., Hatton, T.A., and Wang, D.I.C., 1999. Cell death from bursting bubbles: role of cell attachment to rising bubbles in sparged reactors. *Biotechnol. Bioeng.* **62**, 468–478.

72. Cherry, R.S. and Kwon, K.-Y., 1990. Transient shear stresses on a suspension cell in turbulence. *Biotechnol. Bioeng*. **36**, 563–571.

73. Wu, J., 1995. Mechanism of animal cell damage associated with gas bubbles and cell protection by medium additives. *J. Biotechnol.* **43**, 81–94.

74. Gore, R.A. and Crowe, C.T., 1989. Effect of particle size on modulating turbulent intensity. *Int. J. Multiphase Flow* **15**, 279–285.

75. Caulet, P.J.C., van der Lans, R.G.J.M., and Luyben, K.Ch.A.M., 1996. Hydrodynamical interactions between particles and liquid flows in biochemical applications. *Chem. Eng. J.* **62**, 193–206.

76. Blackshear, P.L. and Blackshear, G.L., 1987. Mechanical hemolysis. In: Skalak, R., Chien, S. (Eds.), *Handbook of Bioengineering.* McGraw-Hill, New York, pp. 15.1–15.19.

77. Garcia-Briones, M.A. and Chalmers, J.J., 1994. Flow parameters associated with hydrodynamic cell injury. *Biotechnol. Bioeng*. **44**, 1089–1098.

78. Chisti, Y. and Moo-Young, M., 1986. Disruption of microbial cells for intracellular products. *Enzyme Microb. Technol*. **8**, 194–204.

79. Taylor, G.I., 1934. The formation of emulsions in definable fields of flow. *Proc. Roy. Soc.* **146**, 501–525.

80. Zhang, Z., Ferenczi, M.A., and Thomas, C.R., 1992. A micromanipulation technique with a theoretical cell model for determining mechanical properties of single mammalian cells. *Chem. Eng. Sci.* **47**, 1347–1354.

81. Lawden, D.F., 1980. *Elliptic Functions and Applications*. Springer-Verlag, New York, pp. 100–102.

82. Abu-Reesh, I. and Kargi, F., 1989. Biological responses of hybridoma cells to defined hydrodynamic shear stress. *J. Biotechnol*. **9**, 167–178.

83. Midler, M. and Finn, R.K., 1966. A model system for evaluating shear in the design of stirred fermentors. *Biotechnol. Bioeng*. **8**, 71–84.

84. Zhong, J.-J., Fujiyama, K., Seki, T., and Yoshida, T., 1994. A quantitative analysis of shear effects on cell suspension and cell culture of *Perilla frutescens* in bioreactors. *Biotechnol. Bioeng*. **44**, 649–654.

85. Doran, P.M., 1993. Design of reactors for plant cells and organs. *Adv. Biochem. Eng. Biotechnol.* **48**, 115–168.

86. Prokop, A., Bajpai, R.K., 1992. The sensitivity of biocatalysts to hydrodynamic shear stress. *Adv. Appl. Microbiol*. **37**, 165–232.

87. Petersen, J.F., McIntire, L.V., and Papoutsakis, E.T., 1990. Shear sensitivity of hybridoma cells in batch, fed-batch, and continuous cultures. *Biotechnol. Prog*. **6**, 114–120.

88. Shiragami, N., 1997. Effect of shear rate on hybridoma cell metabolism. *Bioprocess Eng*. **16**, 345–347.

89. Abu-Reesh, I. and Kargi, F., 1991. Biological responses of hybridoma cells to hydrodynamic shear in an agitated bioreactor. *Enzyme Microb. Technol*. **13**, 913–919.

90. Kioukia, N., Nienow, A.W., Al-Rubeai, M., and Emery, A.N., 1996. Influence of agitation and sparging on the growth rate and infection of insect cells in bioreactors and a comparison with hybridoma culture. *Biotechnol. Prog*. **12**, 779–785.

91. Cook, J.A. and Mitchell, J.B., 1989. Viability measurements in mammalian cell systems. *Anal. Biochem*. **179**, 1–7.

92. Cherry, R.S. and Papoutsakis, E.T., 1988. Physical mechanisms of cell damage in microcarrier cell culture bioreactors. *Biotechnol. Bioeng*. **32**, 1001–1014.

93. McQueen, A. and Bailey, J.E., 1989. Influence of serum level, cell line, flow type and viscosity on flow-induced lysis of suspended mammalian cells. *Biotechnol. Lett.* **11**, 531–536.

94. Ramirez, O.T. and Mutharasan, R., 1992. Effect of serum on the plasma membrane fluidity of hybridomas: an insight into its shear protective mechanism. *Biotechnol. Prog.* **8**, 40–50.

95. Goldblum, S., Bae, Y.-K., Hink, W.F., and Chalmers, J.J., 1990. Protective effect of methyl cellulose and other polymers on insect cells subjected to laminar shear stress. *Biotechnol. Prog*. **6**, 383–390.

96. Kunas, K.T. and Papoutsakis, E.T., 1990. The protective effect of serum against hydrodynamic damage of hybridoma cells in agitated and surface-aerated bioreactors. *J. Biotechnol.* **15**, 57–70.

97. Al-Rubeai, M., Singh, R.P., Goldman, M.H., and Emery, A.N., 1995. Death mechanisms of animal cells in conditions of intensive agitation. *Biotechnol. Bioeng*. **45**, 463–472.

98. Al-Rubeai, M., Singh, R.P., Emery, A.N., and Zhang, Z., 1995. Cell-cycle and cell-size dependence of susceptibility to hydrodynamic-forces. *Biotechnol. Bioeng*. **46**, 88–92.

99. Butler, M., Huzel, N., Barnabé, N., Gray, T., and Bajno, L., 1999. Linoleic acid improves the robustness of cells in agitated cultures. *Cytotechnology* **30**, 27–36.

100. Palomares, L.A., González, M., Ramírez, O.T., 2000. Evidence of Pluronic F-68 direct interaction with insect cells: impact on shear protection, recombinant protein, and baculovirus production. *Enzyme Microb. Technol.* **26**, 324–331.

101. Kim, B.-Y., Putnam, A.J., Kulik, T.J., and Mooney, D.J., 1998. Optimizing seeding and culture methods to engineer smooth muscle tissue on biodegradable polymer matrices. *Biotechnol. Bioeng*. **57**, 46–54.

102. Hochmuth, R.M., 1987. Properties of red blood cells. In: Skalak, R., Chien, S. (Eds.), *Handbook of Bioengineering*. McGraw-Hill, New York, pp. 12.1–12.17.

103. Zhang, Z., Chisti, Y., and Moo-Young, M., 1995. Effects of the hydrodynamic environment and shear protectants on survival of erythrocytes in suspension. *J. Biotechnol.* **43**, 33–40.

104. Ramírez, O.T. and Mutharasan, R., 1990. The role of the plasma membrane fluidity on the shear sensitivity of hybridomas grown under hydrodynamic stress. *Biotechnol. Bioeng.* **36**, 911–920.

105. Schmid-Schönbein, G.W., 1987. Rheology of leukocytes. In: Skalak, R., Chien, S. (Eds.), *Handbook of Bioengineering*. McGraw-Hill, New York, pp. 13.1–13.25.

106. Chittur, K.K., McIntire, L.V., and Rich, R.R., 1988. Shear stress effects on human T cell function. *Biotechnol. Prog.* **4**(2), 89–96.

107. Olivier, L.A. and Truskey, G.A., 1993. A numerical analysis of forces exerted by laminar flow on spreading cells in a parallel plate flow chamber assay. *Biotechnol. Bioeng*. **42**, 963–973.

108. Sirois, E., Charara, J., Ruel, J., Dussault, J.C., Gagnon, P., and Doillon, C.J., 1998. Biomaterials 19, 1925–1934. Endothelial cells exposed to erythrocytes under shear stress: an *in vitro* study.

109. Papadaki, M. and Eskin, S.G., 1997. Effects of fluid shear stress on gene regulation of vascular cells. *Biotechnol. Prog*. **13**, 209–221.

110. Ziegelstein, R.C., Cheng, L., and Capogrossi, M.C., 1992. Flow-dependent cytosolic acidification of vascular endothelial cells. *Science* 258, 656–659.

111. Niebauer, J., Dulak, J., Chan, J.R., Tsao, P.S., and Cooke, J.P., 1999. Gene transfer of nitric oxide synthase: Effects on endothelial biology. *J. Am. Coll. Cardiol*. 34, 1201–1207.

112. Lakhotia, S., Bauer, K.D., and Papoutsakis, E.T., 1993. Fluid-mechanical forces in agitated bioreactors reduce the CD13 and CD33 surface proteins content of HL60 cells. *Biotechnol. Bioeng*. **41**, 868–877.

113. Shiragami, N. and Unno, H., 1994. Effect of shear stress on activity of cellular enzyme in animal cell. *Bioprocess Eng.* **10**, 43–45.

114. Dai, X., Ouyang, F., and Qi, Y., 1994. Preliminary investigation on anchorage-dependent cell culture by air-lift suspending microcarriers. In: Teo, W.K., Yap, M.G.S., Oh, S.K.W. (Eds.), *Better Living Through Biochemical Engineering.* University of Singapore, Singapore, pp. 408–410.

115. Cherry, R.S. and Papoutsakis, E.T., 1986. Hydrodynamic effects on cells in agitated tissue culture reactors. *Bioprocess Eng*. 1, 29–41.

116. Venkat, R.V., Stock, L.R. and Chalmers, J.J., 1996. Study of hydrodynamics in microcarrier culture spinner vessels: a particle tracking velocimetry approach. *Biotechnol. Bioeng*. 49, 456–466.

117. Chisti, Y. and Moo-Young, M., 1993. Effectively use fragile biocatalysts in bioreactors. *Chimica Oggi* **11**(3–4), 25–27.

118. Cherry, R.S., 1993. Animal cells in turbulent fluids: Details of the physical stimulus and the biological response. *Biotechnol. Adv.* **11**, 279–299.

119. Toshisuke, M., Hiroki, K., Koji, M., Masao, Y., and Yoshio, Y., 1993. Disruption of cytoskeletal structures mediates endotheline-1 gene expression in cultured porcine aortic endothelial cells. *J. Clin. Invest*. **92**, 1706–1712.

120. Zhang, Z., Ferenczi, M.F., Lush, A.C., and Thomas, C.R., 1991. A novel micromanipulation technique for measuring the bursting strength of single mammalian cells. *Appl. Microbiol. Biotechnol*. **36**, 208–210.

121. Sinskey, A.J., Fleishaker, R.J., Tyo, M.A., Giard, D.-J., and Wang, D.I.C., 1981. Production of cell-derived products: virus and interferon. *Ann. N. Y. Acad. Sci.* **369**, 47–59.

122. Ganzeveld, K.J., Chisti, Y., and Moo-Young, M., 1995. Hydrodynamic behaviour of animal cell microcarrier suspensions in split-cylinder airlift bioreactors. *Bioprocess Eng*. **12**, 239–247.

123. Wang, Y. and Ouyang, F., 1999. Bead-to-bead transfer of Vero cells in microcarrier culture. *Bioprocess Eng*. **21**, 211–213.

124. Yamamoto, A., Mishima, S., Maruyama, N., and Sumita, M., 1998. A new technique for direct measurement of the shear force necessary to detach a cell from a material. *Biomaterials* **19**, 871–879.

125. Wu, S.-C., 1999. Influence of hydrodynamic shear stress on microcarrier-attached cell growth: Cell line dependency and surfactant protection. *Bioprocess Eng*. **21**, 201–206.

126. Williams, A.R., 1973. Viscoelasticity of the human erythrocyte membrane. *Biorheology* **10**, 313–319.

127. Suzuki, T., Matsuo, T., Ohtaguchi, K., and Koide, K., 1995. Gas-sparged bioreactors for CO_2 fixation by *Dunaliella tertiolecta*. *J. Chem. Technol. Biotechnol*. **62**, 351–358.

128. Lakhotia, S., Bauer, K.D., and Papoutsakis, E.T., 1992. Damaging agitation intensities increase DNA-synthesis rate and alter cell-cycle phase distributions of CHO cells. *Biotechnol. Bioeng.* **40**, 978–990.